Instituto Argentino de Radioastronomía

ISSN: 1853-5461

Black hole astrophysics

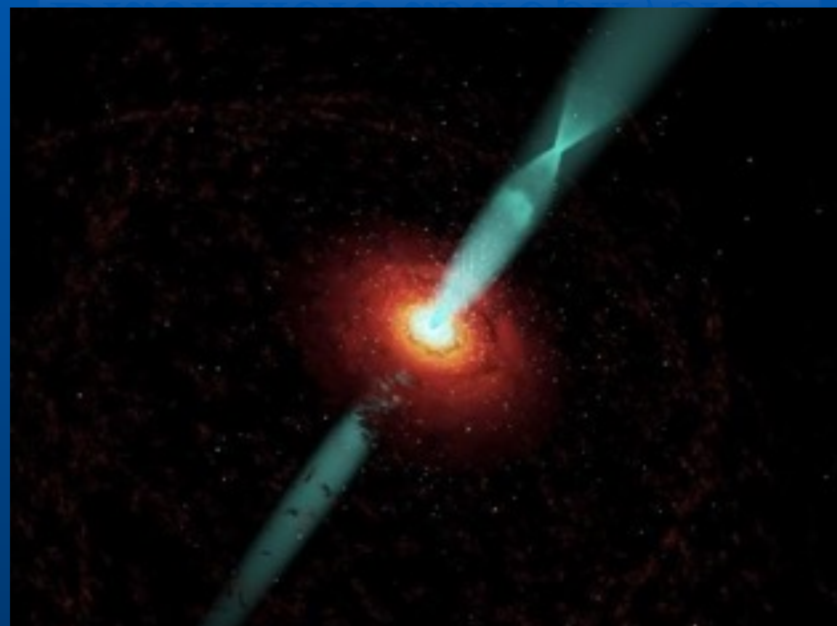

Gustavo E. Romero

Grupo de Astrofísica Relativista y Radioastronomía

Instituto Argentino de Radioastronomía, CONICET

Facultad de Ciencias Astronómicas y Geofísicas, UNLP

romero@iar-conicet.gov.ar, romero@fcaglp.unlp.edu.ar

Jets

Jets are collimated outflows observed in a variety of astrophysical situations. The most spectacular examples are related to disk accretion onto a compact object.

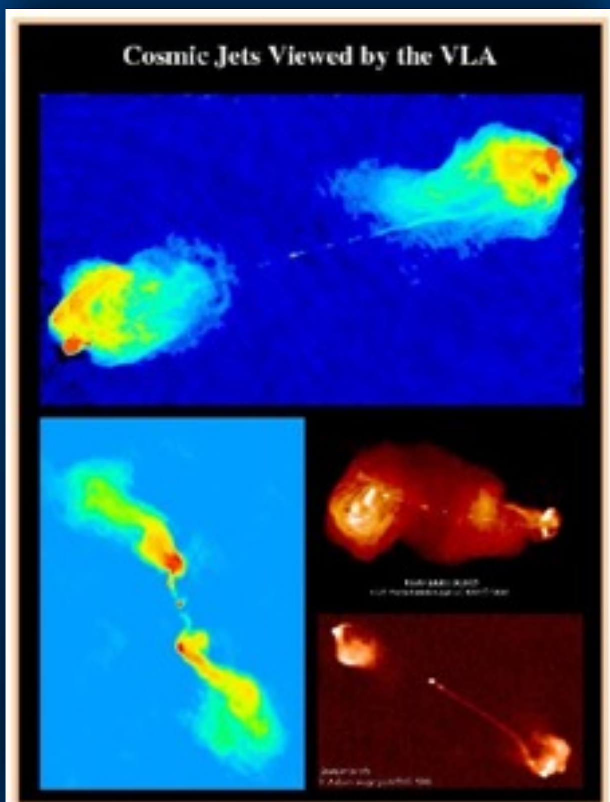

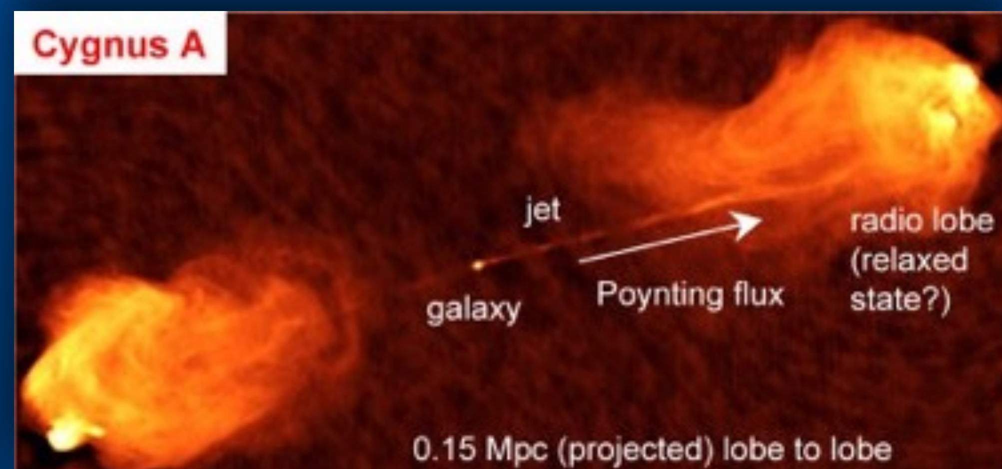

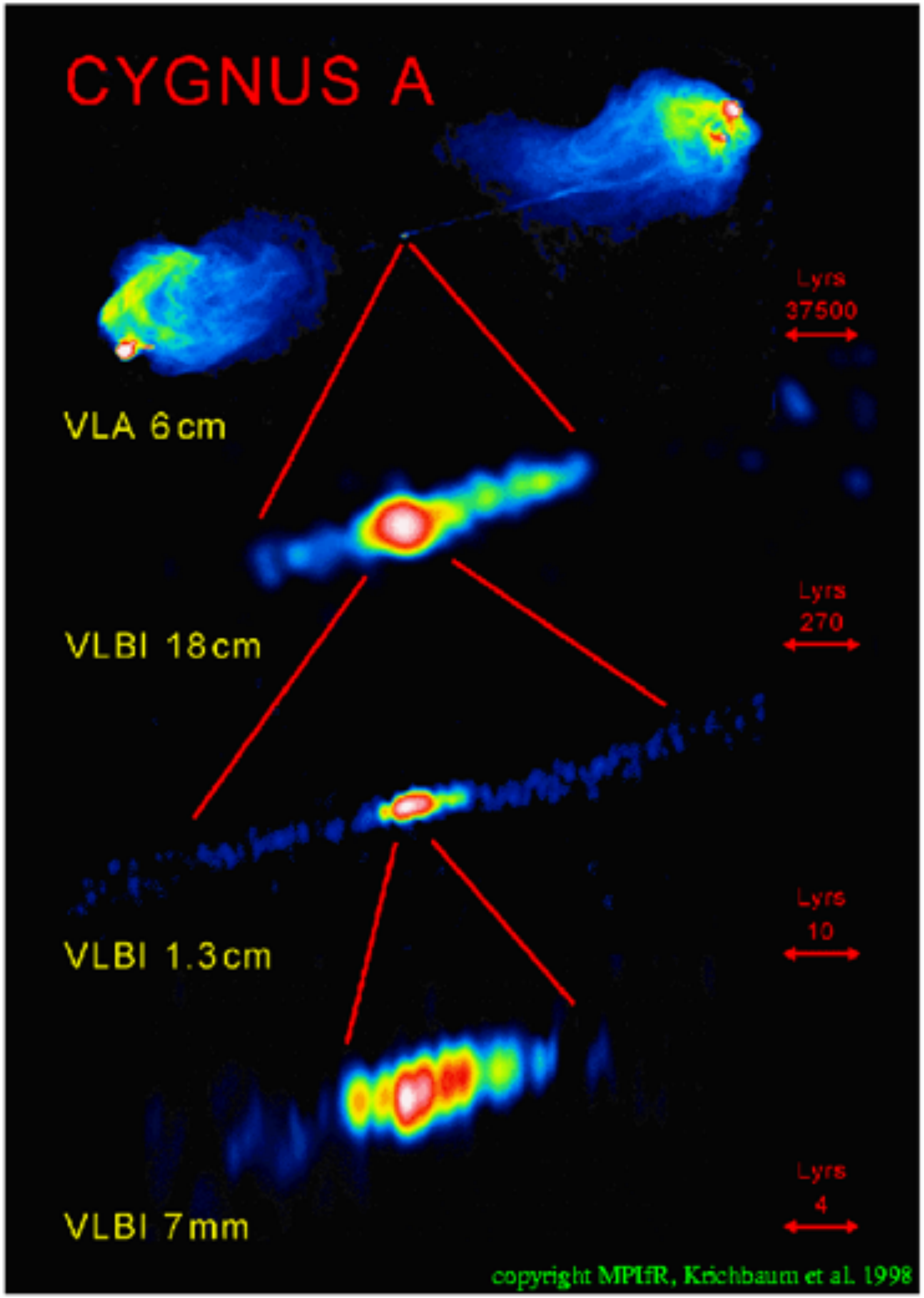
CYGNUS A
VLA 6cm
Lyrs
37500
VLBI 18cm
Lyrs
270
VLBI 1.3cm
Lyrs
10
VLBI 7mm
Lyrs
4
copyright MPIfR, Krichbaum et al. 1998

CYGNUS A - VLA, 6cm

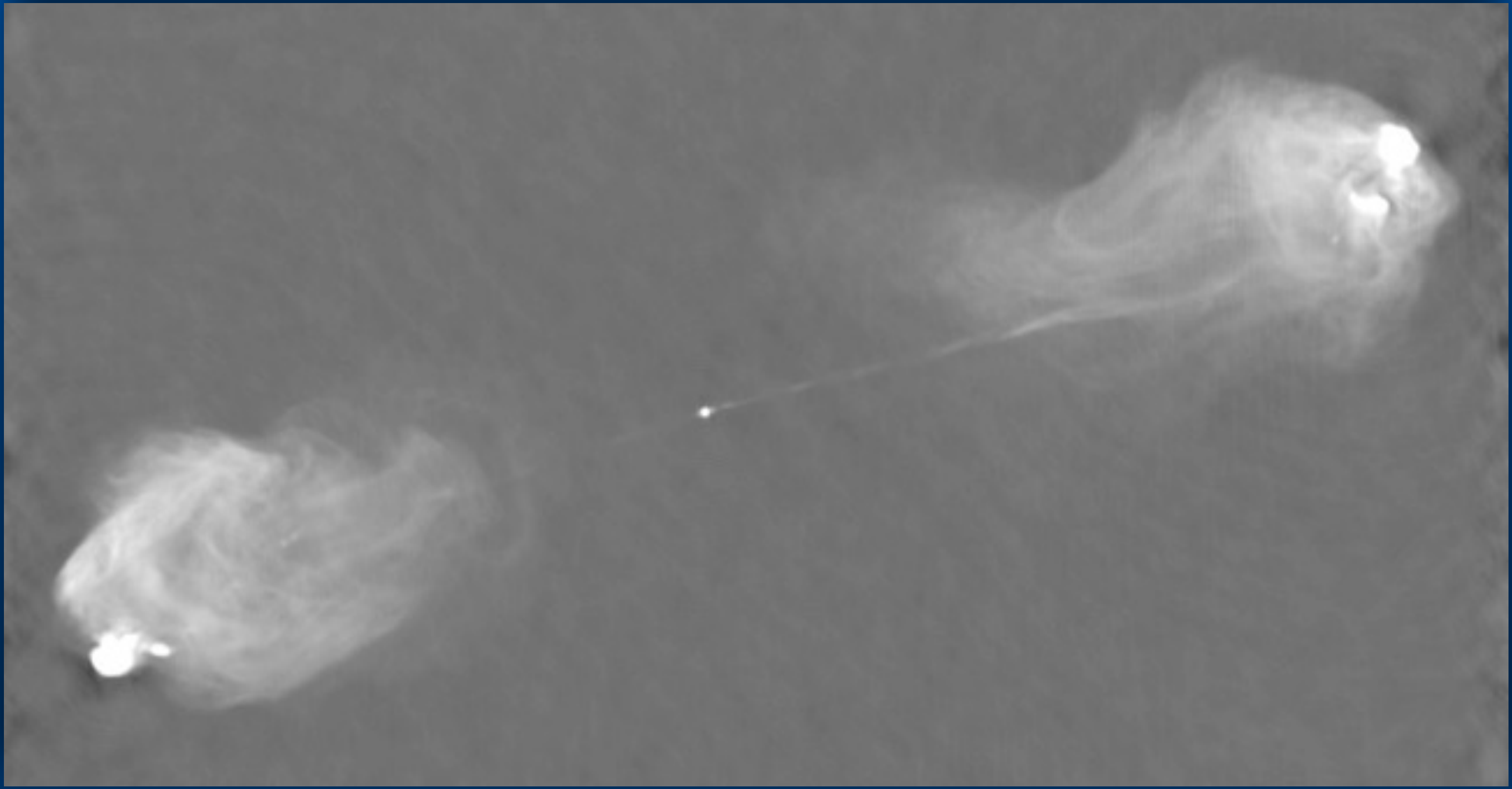

CYGNUS A - VLA, 6cm

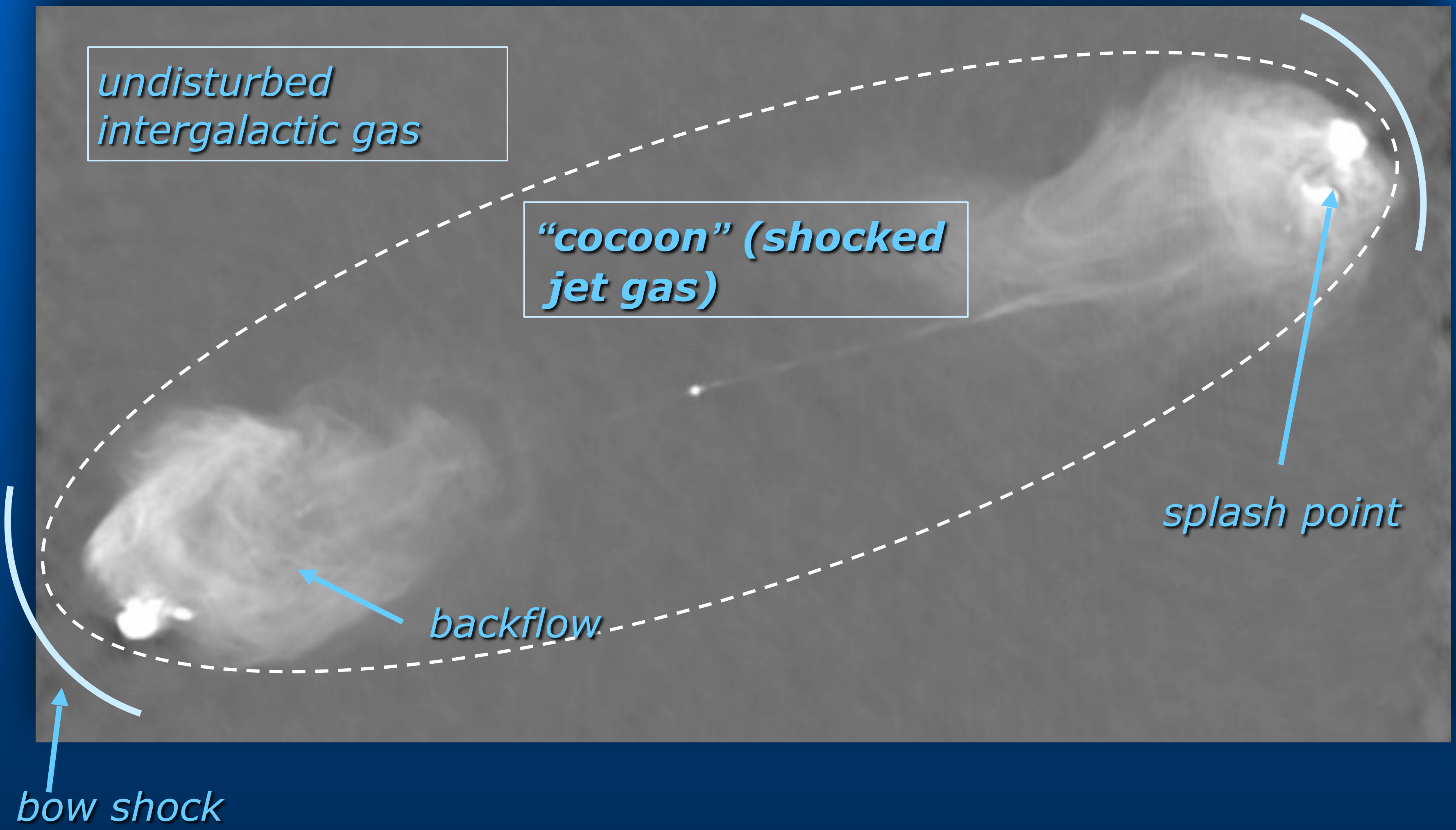

Microquasar GRS 1758−258 (Martí, Luque-Escamilla, Romero, et al. , A&A, 2015).

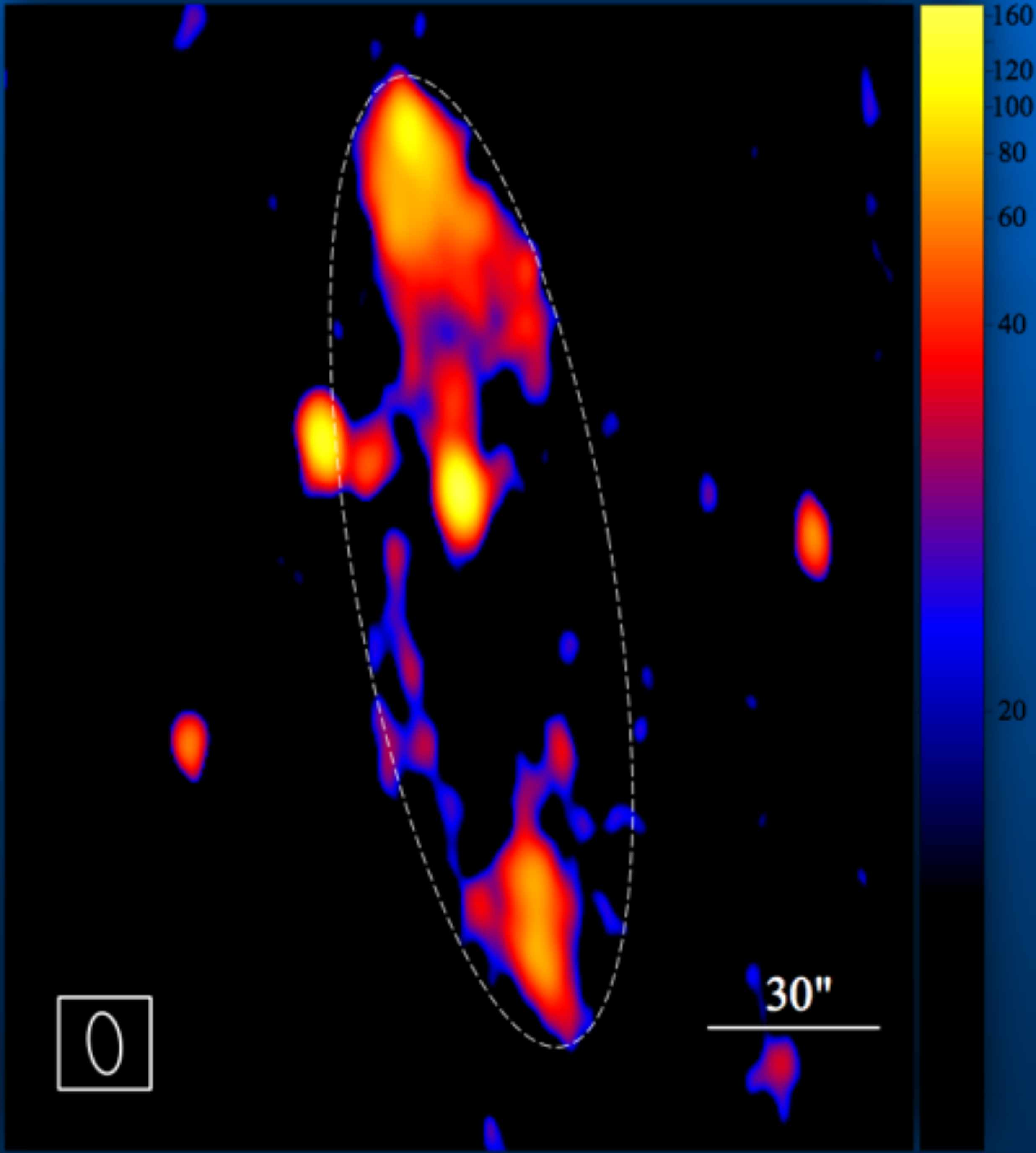

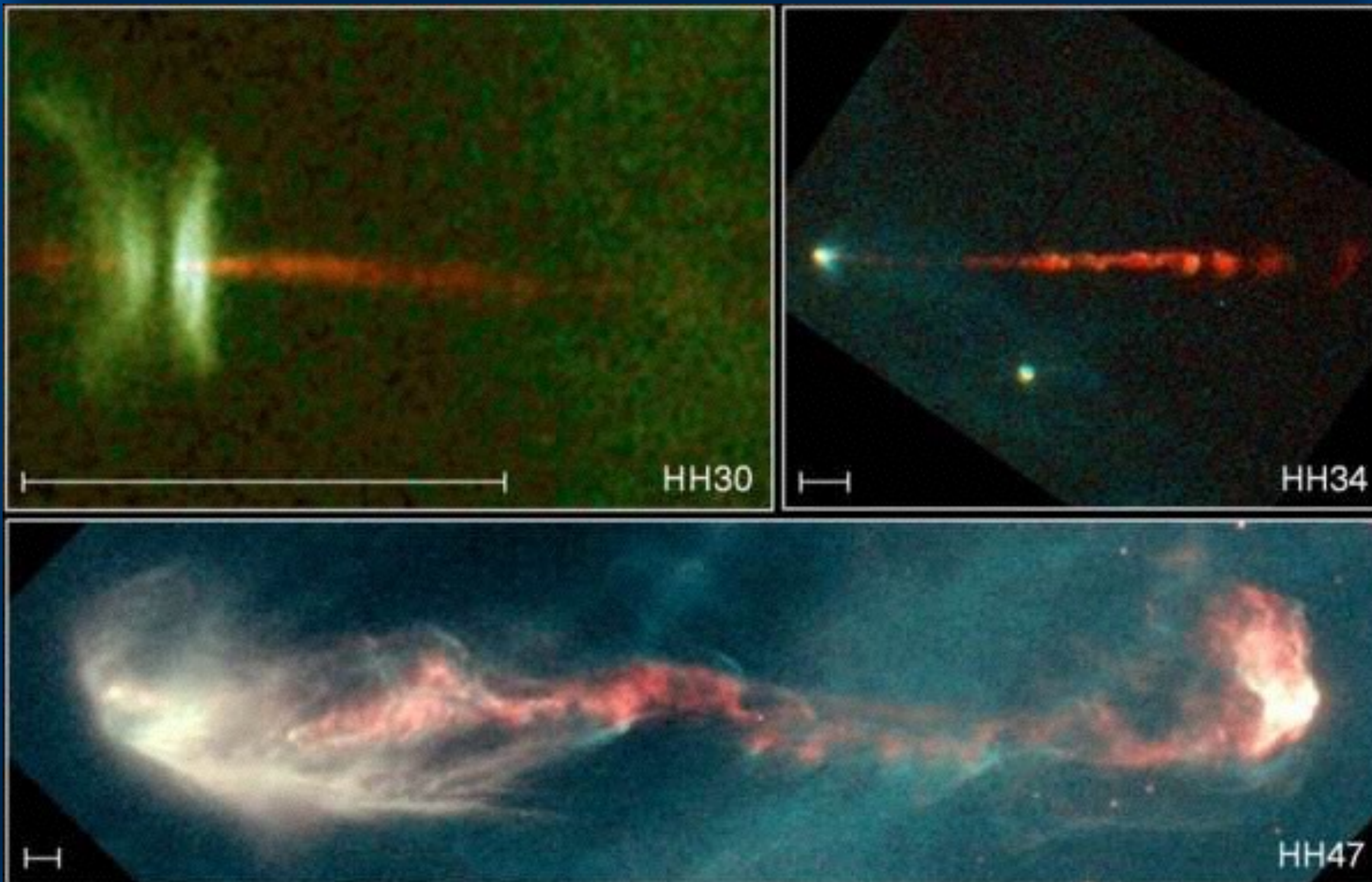
HH30
HH34
HH47

3C120

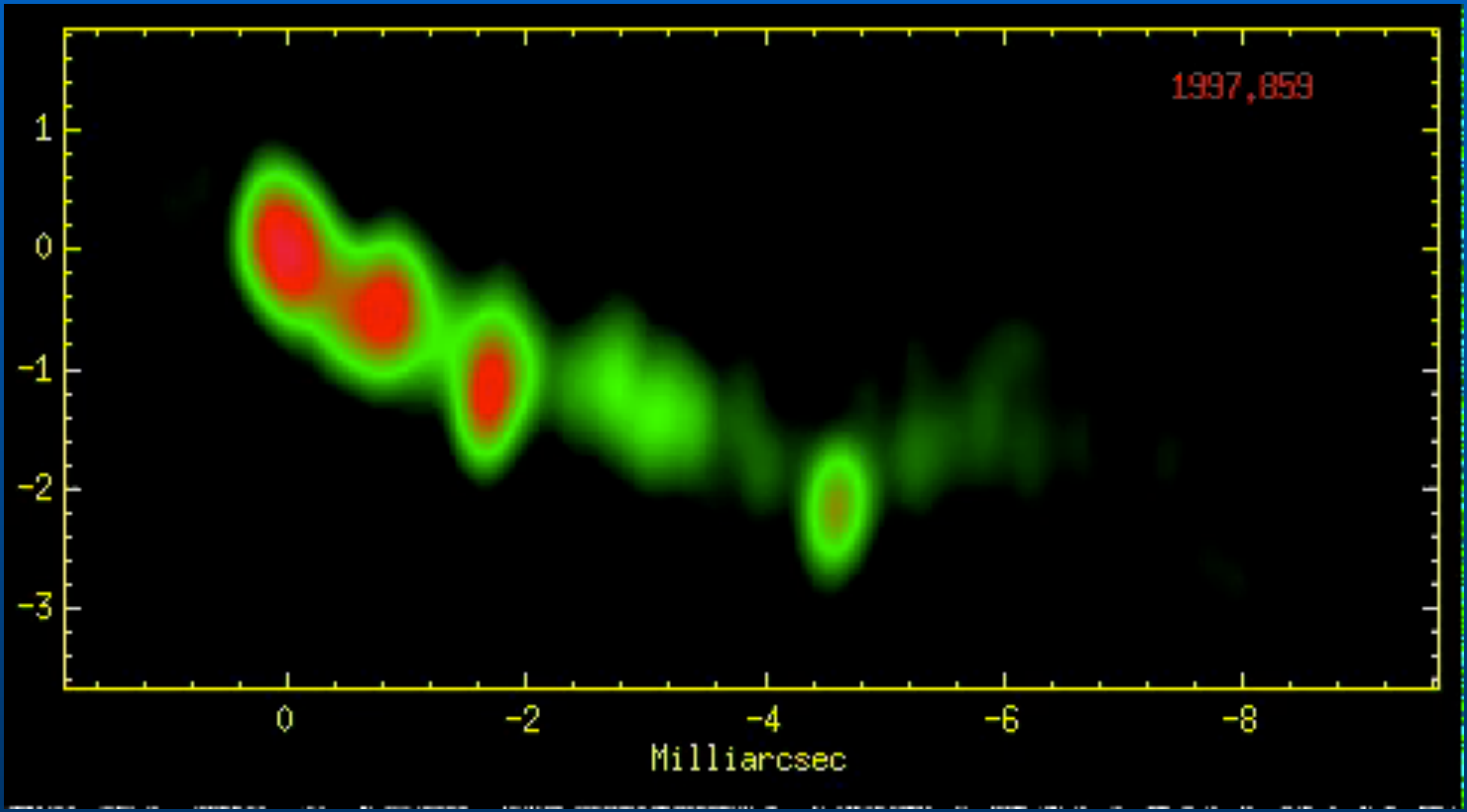

MOVIE

QUASAR 3C 279
FROM RADIO TO X-RAYs

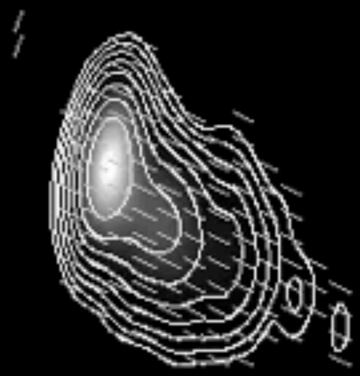

ALAN MARSCHER /BU
SVETLANA JORSTAD /BU
MARGO ALLER /UMRAO
TOMATH BALONEK /COLGATE U.
IAN McHARDY /U. of SOUTHAMPTON

The hot spot moves 13’’ in 5.4 yr, impying v ~ 0,32c

The hot spot is destroyed

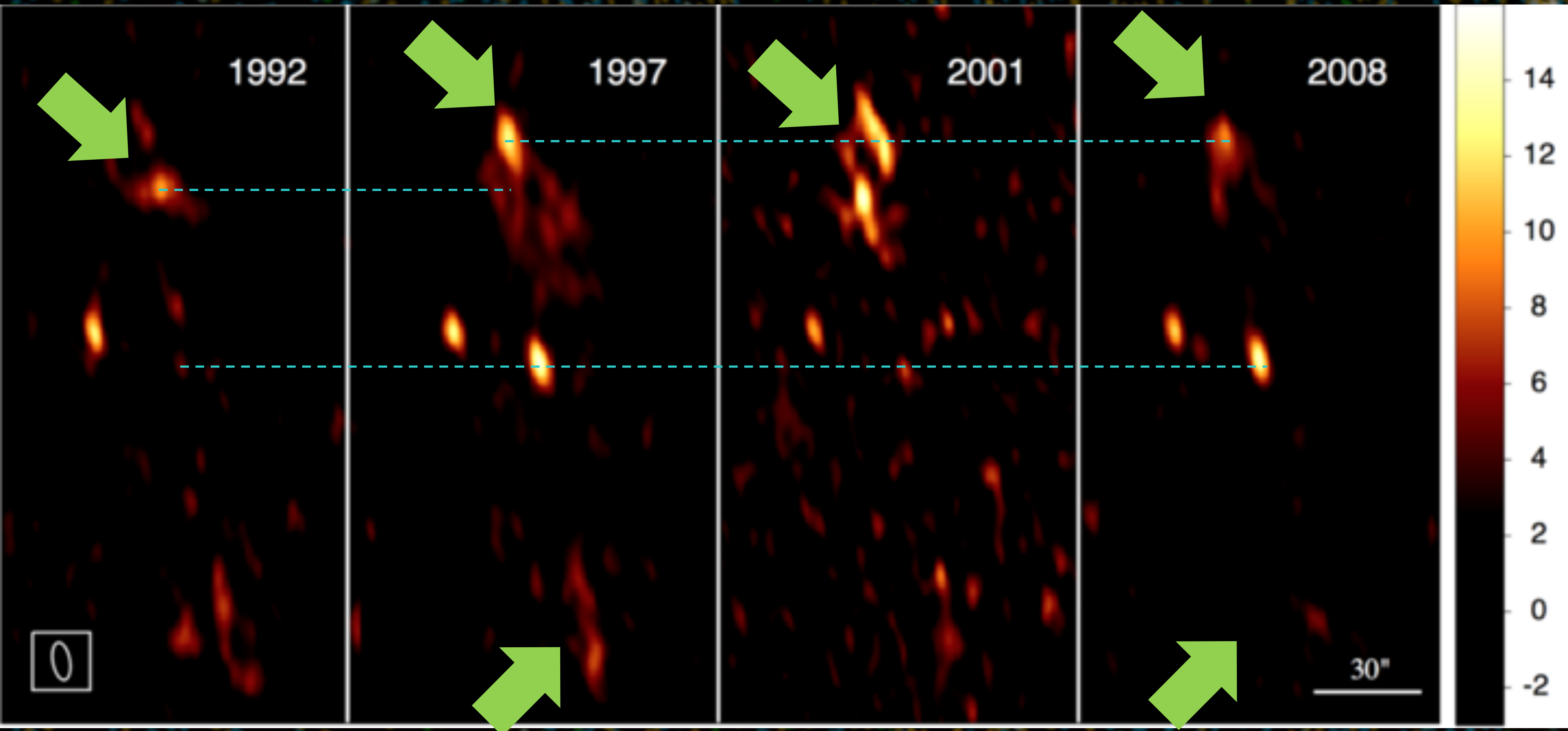

The southern lobe is much weaker and disappears in 2008.

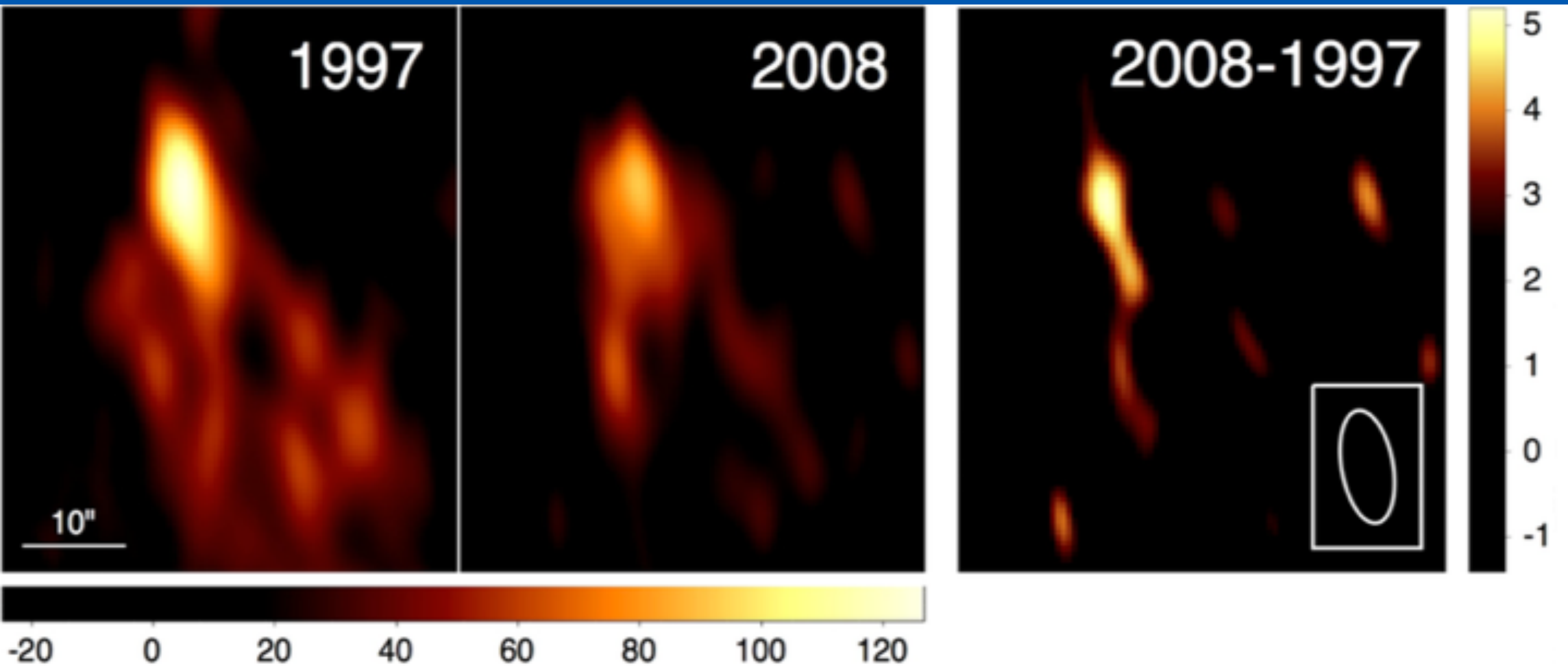

1997
2008
2008-1997
10"
-20
0
20
40
60
80
100
120
5
4
3
2
1
0
-1

Acceleration: pressure (gas)

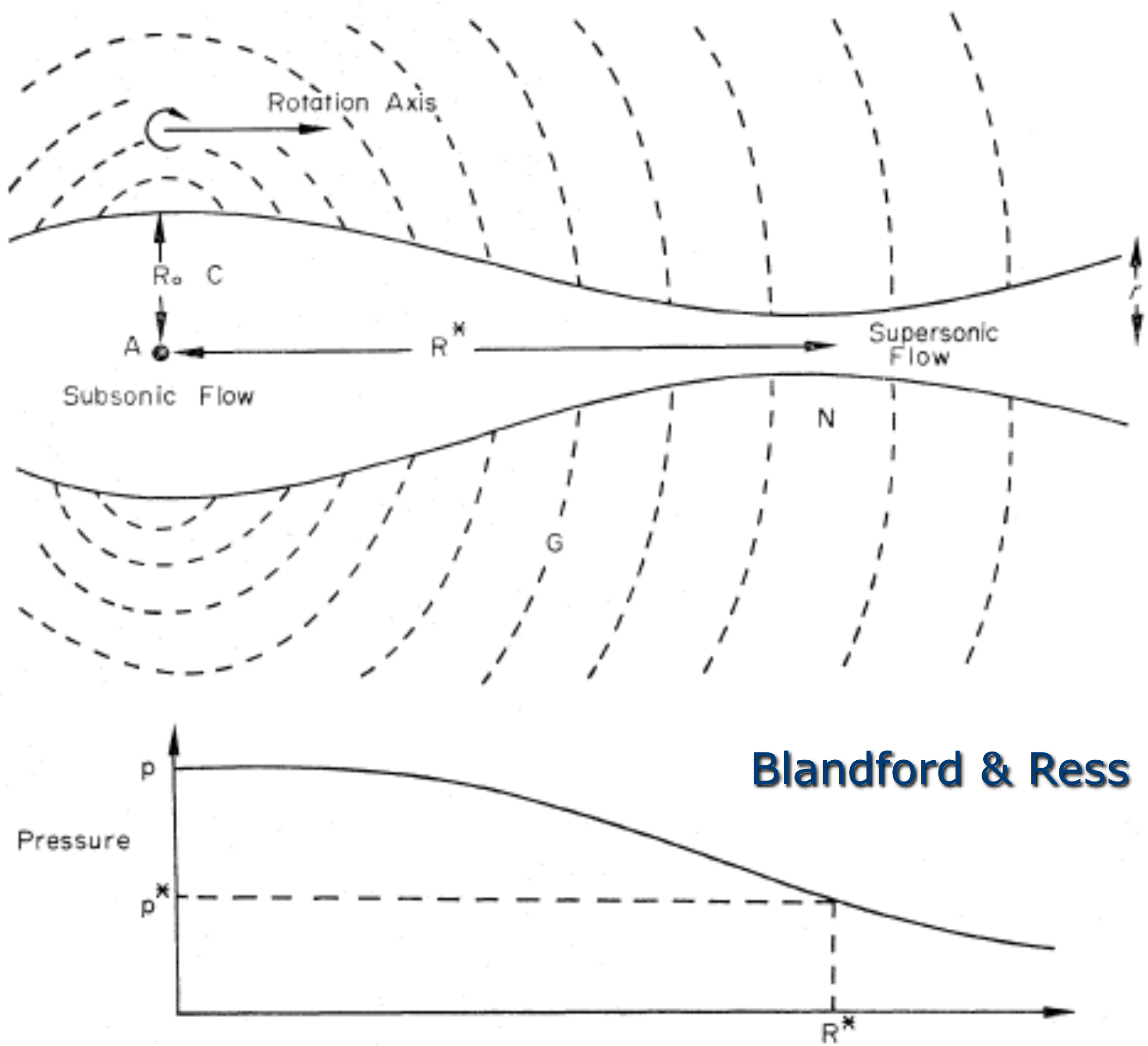

Blandford & Ress 1974

Acceleration: pressure (radiation)

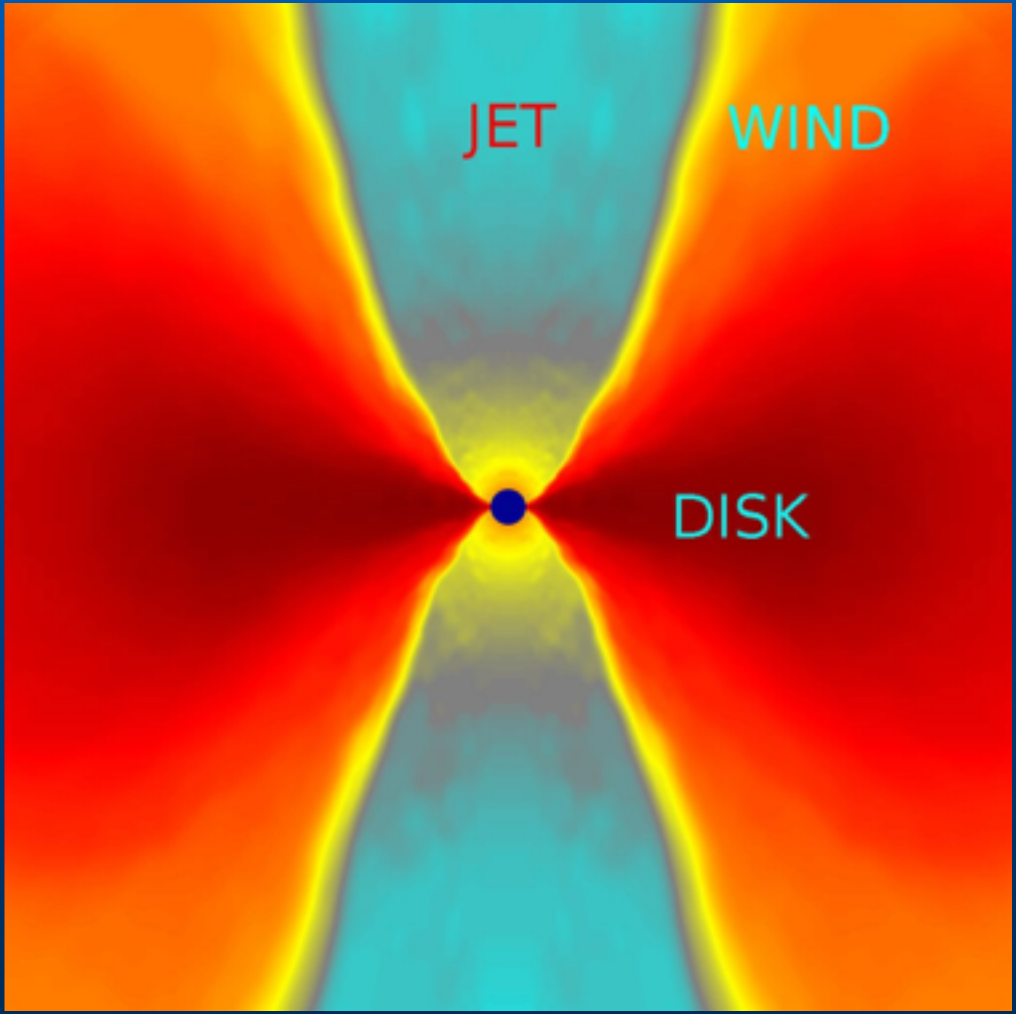

In *non-relativistic* MHD the relevant field is the magnetic field $\mathbf{B}$. Indeed, if the velocity of the flow is $v \ll c$ everywhere, it can be shown that $|\mathbf{E}| \ll |\mathbf{B}|$. This also means that the displacement current may be ignored, so that

$$\nabla \times \mathbf{B} = \frac{4\pi}{c}\mathbf{J}$$

$$\mathbf{f}_{\mathrm{L}} = \frac{\mathbf{J} \times \mathbf{B}}{c} = \frac{1}{4\pi}(\nabla \times \mathbf{B}) \times \mathbf{B}.$$

$$\mathbf{J} = \sigma\left(\mathbf{E} + \frac{\mathbf{v}}{c} \times \mathbf{B}\right),$$

$$\nabla \cdot \mathbf{B} = 0,$$

$$\nabla \times \mathbf{E} = -\frac{1}{c}\frac{\partial \mathbf{B}}{\partial t},$$

$$\nabla \cdot \mathbf{E} = 4\pi \rho_{\mathrm{e}}.$$

Induction equation for B

$$\frac{\partial \mathbf{B}}{\partial t} = \nabla \times (\mathbf{v} \times \mathbf{B}) + \frac{c^2}{4\pi\sigma}\nabla^2 \mathbf{B}.$$

The induction equation states that the magnetic field at a given point in space varies in time because it is advected with the flow (first term on the right-hand side) and because it diffuses (second term on the right-hand side).

$$\frac{\partial \rho}{\partial t} + \nabla \cdot (\rho \mathbf{v}) = 0,$$

$$\rho \left[\frac{\partial \mathbf{v}}{\partial t} + (\mathbf{v} \cdot \nabla) \mathbf{v} \right] = -\nabla P - \rho \nabla \Phi + \frac{1}{4\pi} (\nabla \times \mathbf{B}) \times \mathbf{B},$$

Steady state ideal non-relativistic MHD equations

$$\nabla \times \mathbf{B} = \frac{4\pi}{c}\mathbf{J},$$

$$\nabla \cdot \mathbf{B} = 0,$$

$$\nabla \times \mathbf{E} = 0,$$

$$\nabla \cdot \mathbf{E} = 4\pi\rho_{\mathrm{e}},$$

$$\mathbf{E} + \frac{1}{c}\mathbf{v} \times \mathbf{B} = 0,$$

$$\nabla \times (\mathbf{v} \times \mathbf{B}) = 0,$$

$$\nabla \cdot (\rho\mathbf{v}) = 0,$$

$$\rho(\mathbf{v} \cdot \nabla)\mathbf{v} = -\nabla P - \rho\nabla\Phi + \frac{1}{4\pi}(\nabla \times \mathbf{B}) \times \mathbf{B}.$$

$$\mathbf{B} = \mathbf{B}_\mathrm{p} + B_\phi \hat{\phi}.$$

$$\mathbf{B}_\mathrm{p} \equiv B_r \hat{r} + B_z \hat{z}$$

$$\nabla \cdot \mathbf{B} = 0,$$

$$\mathbf{B}_\mathrm{p} = \nabla \times \left(\frac{\Psi}{r} \hat{\phi} \right) = \frac{1}{r} \nabla \Psi \times \hat{\phi},$$

flux function or *stream function* Ψ

$$\mathbf{B}_r = -\frac{1}{r} \frac{\partial \Psi}{\partial z}, \qquad \mathbf{B}_z = \frac{1}{r} \frac{\partial \Psi}{\partial r}.$$

$$\mathbf{B} \cdot \nabla \Psi = \mathbf{B}_\mathrm{p} \cdot \nabla \Psi = 0,$$

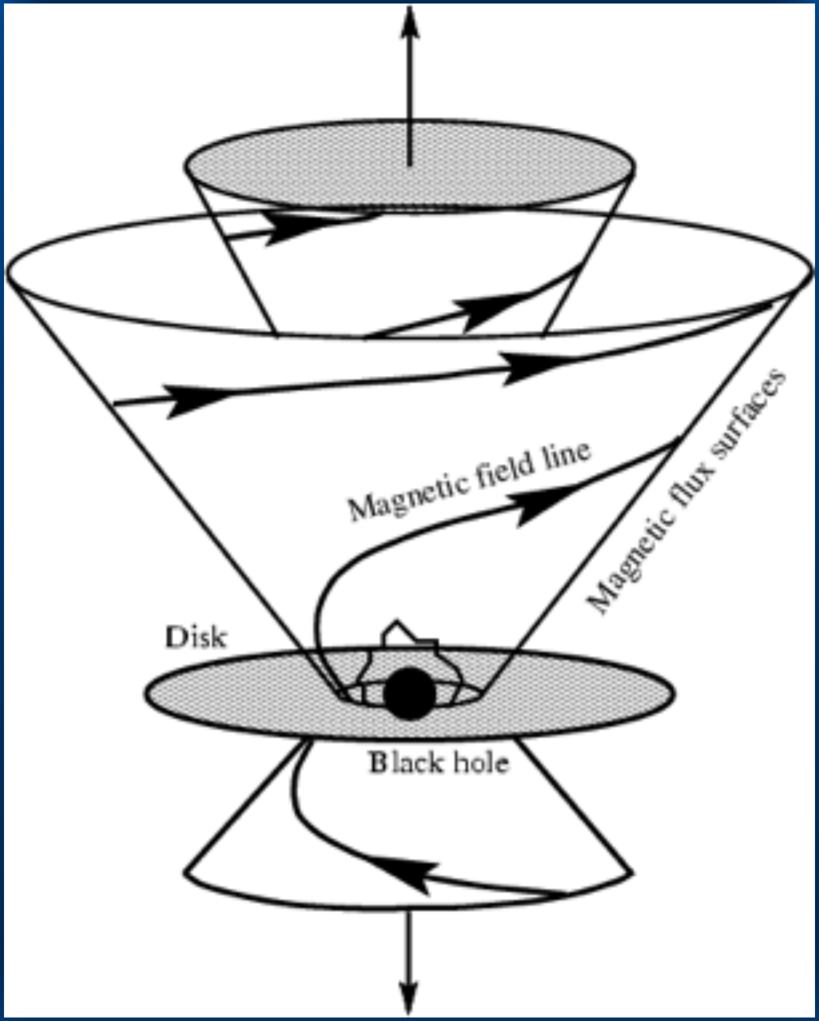

Ψ is constant along magnetic field lines. Equivalently, the vectors $\mathbf{B}$ and $\mathbf{B}_p$ lie on surfaces where Ψ = constant; these are called *magnetic surfaces*.

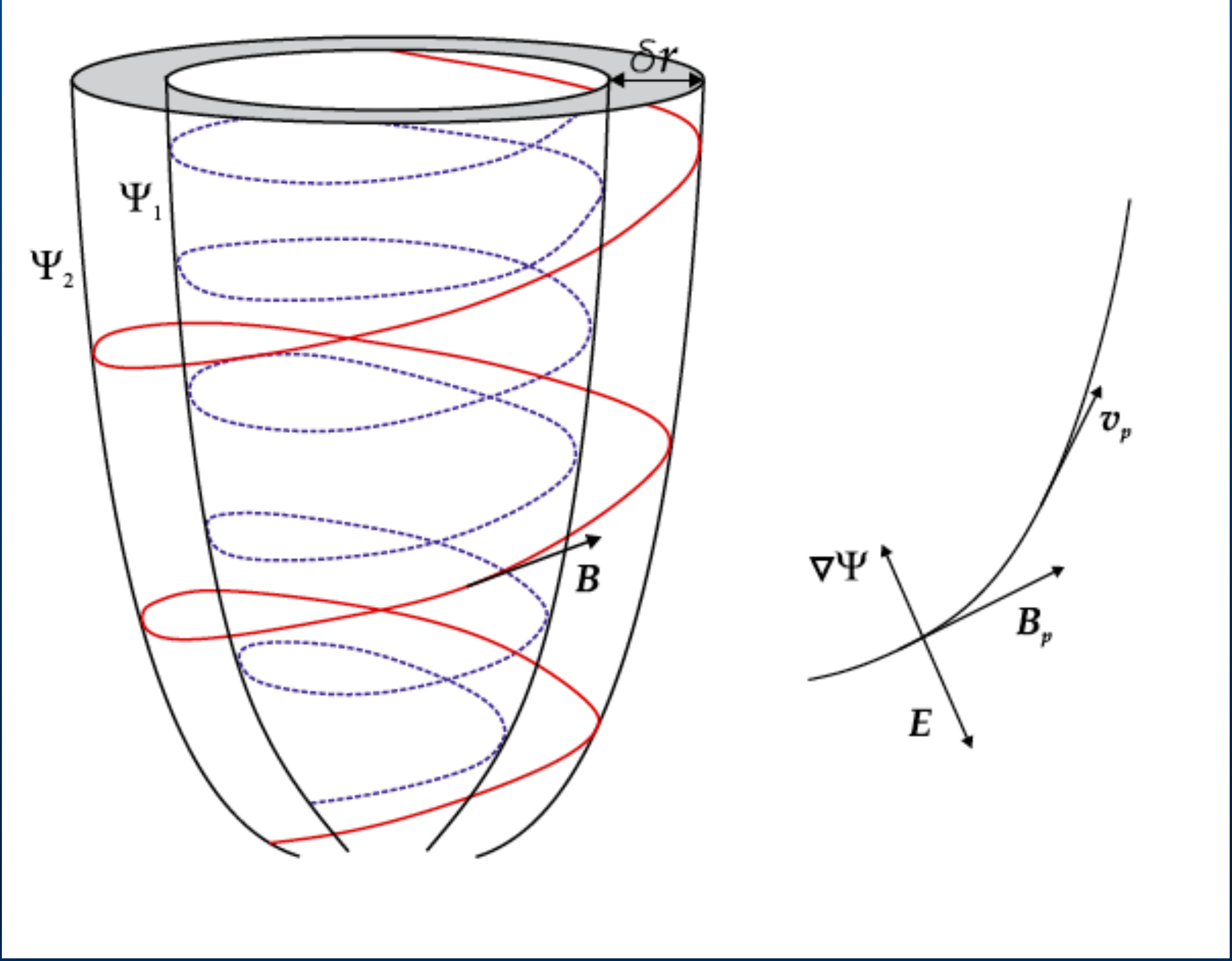

δr
Ψ_1
Ψ_2
B
v_p
$\nabla\Psi$
B_p
E

$$\frac{\rho v_{\mathrm{p}}}{B_{\mathrm{p}}} = \eta(\Psi)$$

$$\eta(\Psi) = \frac{d\Psi_{\mathrm{m}}}{d\Psi},$$

Mass load function

$$d\Psi_{\mathrm{m}} = \rho v_{\mathrm{p}} dA \text{ and } d\Psi = B_{\mathrm{p}} dA$$

Mach-Alfvén number

$$M_{\mathrm{A}}^2 \equiv \frac{v_{\mathrm{p}}^2}{v_{\mathrm{Ap}}^2},$$

Alfvén velocity

$$\mathbf{v}_{\mathrm{A}} \equiv \frac{\mathbf{B}}{\sqrt{4\pi\rho}}.$$

The *Alfvén radius* r_{A} is the point on each poloidal field line where $M_{\mathrm{A}} = 1$; the loci of all r_{A} define the *Alfvén surface*.

Poloidal component of the Poynting vector

$$\mathbf{S}_{\mathrm{p}} = \frac{c}{4\pi}(\mathbf{E} \times \mathbf{B})_{\mathrm{p}} = -\frac{r\Omega B_{\phi}}{4\pi}\mathbf{B}_{\mathrm{p}},$$

Grad-Shafranov equation

The Grad–Shafranov equation is the equilibrium equation in ideal MHD for a two dimensional plasma. This equation is a two-dimensional, nonlinear, elliptic partial differential equation obtained from the reduction of the ideal MHD equations to two dimensions, for the case of toroidal axisymmetry.

$$\nabla \cdot \left[(M_{\mathrm{A}} - 1) \frac{\nabla \Psi}{4\pi r^2} \right] - \left(B_\phi^2 + M_{\mathrm{A}}^2 B_{\mathrm{p}}^2 \right) \frac{\eta'}{4\pi \eta}$$

The primes indicate derivatives with respect to the flux function Ψ

$$= \rho \left[E' - \Omega_{\mathrm{m}} (\Omega r_{\mathrm{A}})' - \left(\Omega_{\mathrm{m}} r^2 - \Omega r_{\mathrm{A}}^2 \right) \Omega' - \frac{a_{\mathrm{s}}^2}{\gamma(\gamma - 1)} K' \right].$$

$$E(\Psi) = \frac{1}{2} v^2 + h + \Phi - \frac{r \Omega B_\phi}{4\pi \eta}.$$

$$h = \gamma a_{\mathrm{s}}^2 / (\gamma - 1).$$

$$P = K \rho^\gamma ,$$

Acceleration: magnetic effects

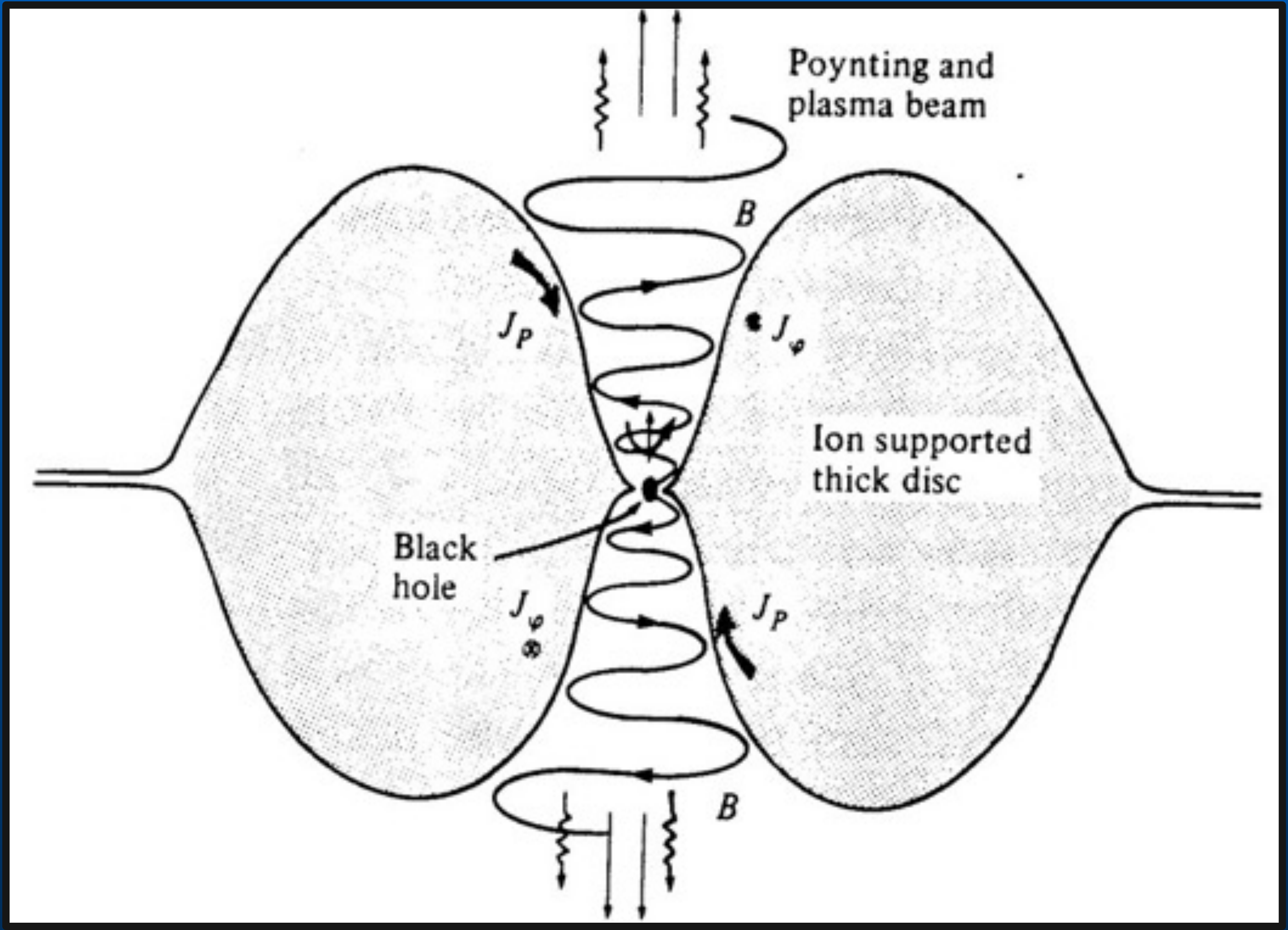

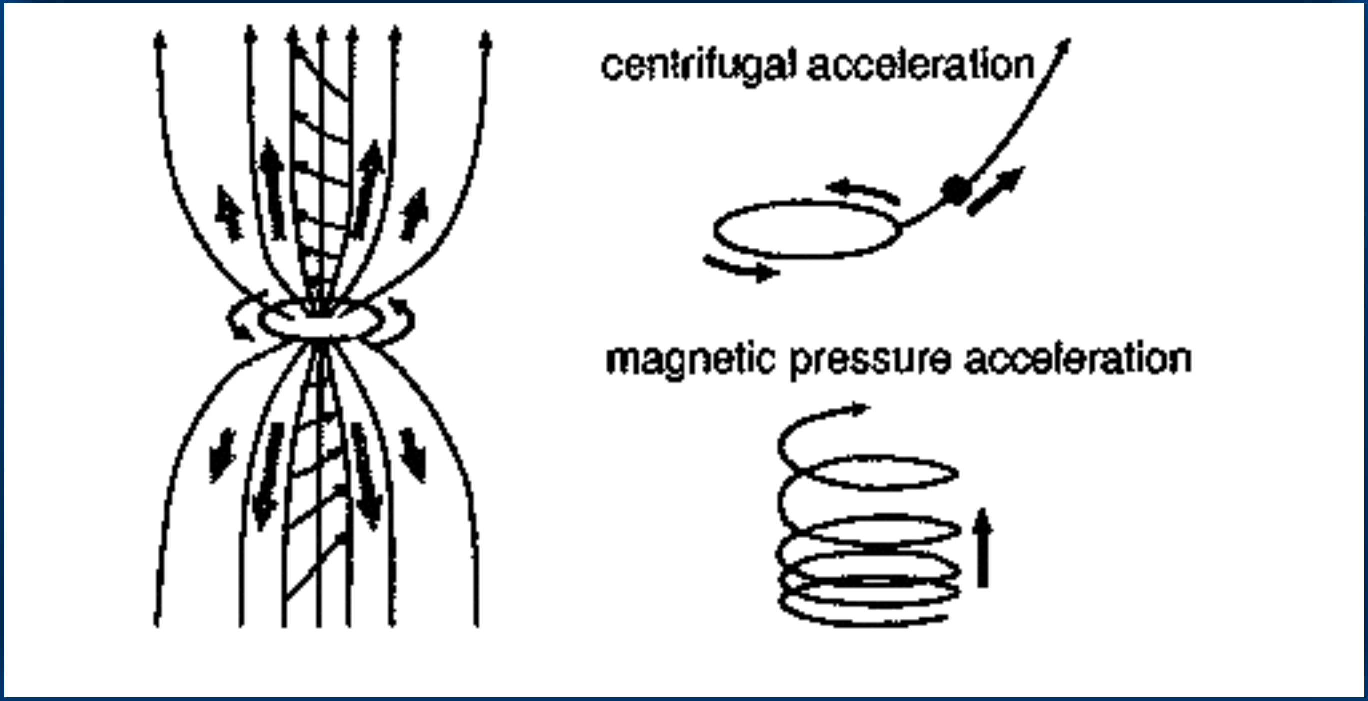
centrifugal acceleration
magnetic pressure acceleration

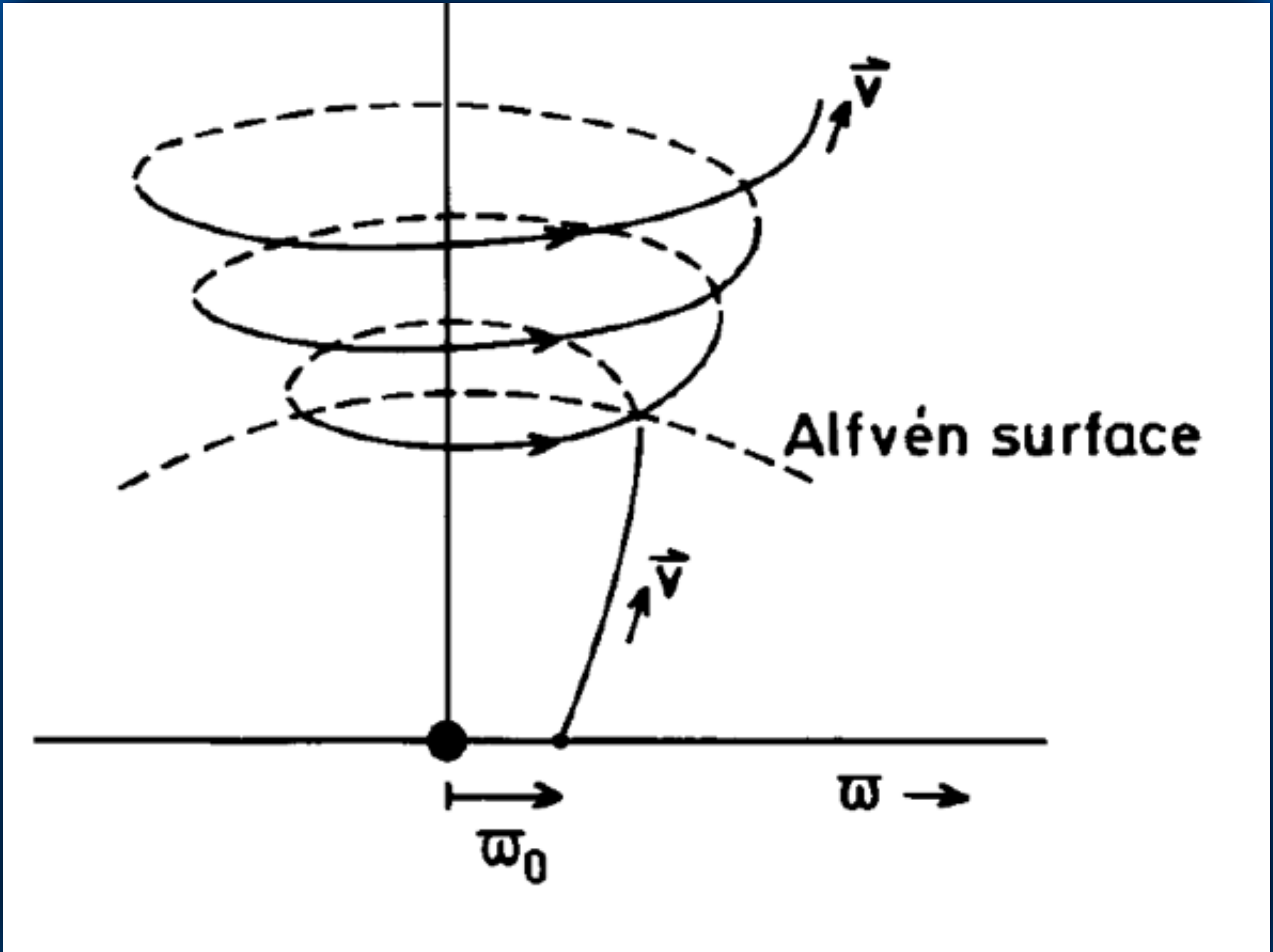

$\vec{v}$
Alfvén surface
$\vec{v}$
$\varpi \rightarrow$
ϖ_0

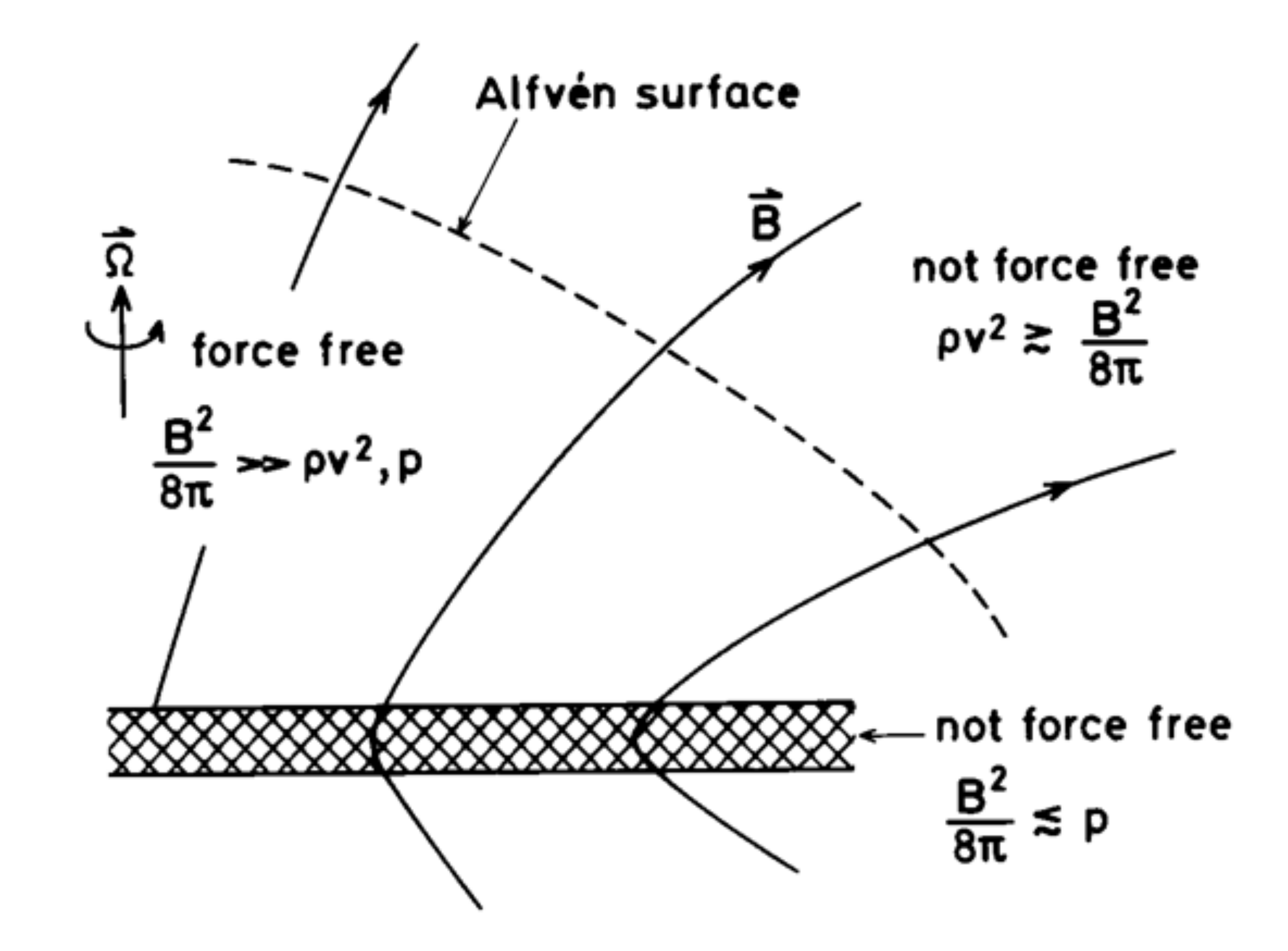
Alfvén surface
$\vec{B}$
$\vec{\Omega}$
not force free
$\rho v^2 \gtrsim \frac{B^2}{8\pi}$
force free
$\frac{B^2}{8\pi} \gg \rho v^2, p$
not force free
$\frac{B^2}{8\pi} \lesssim p$

Magnetic acceleration

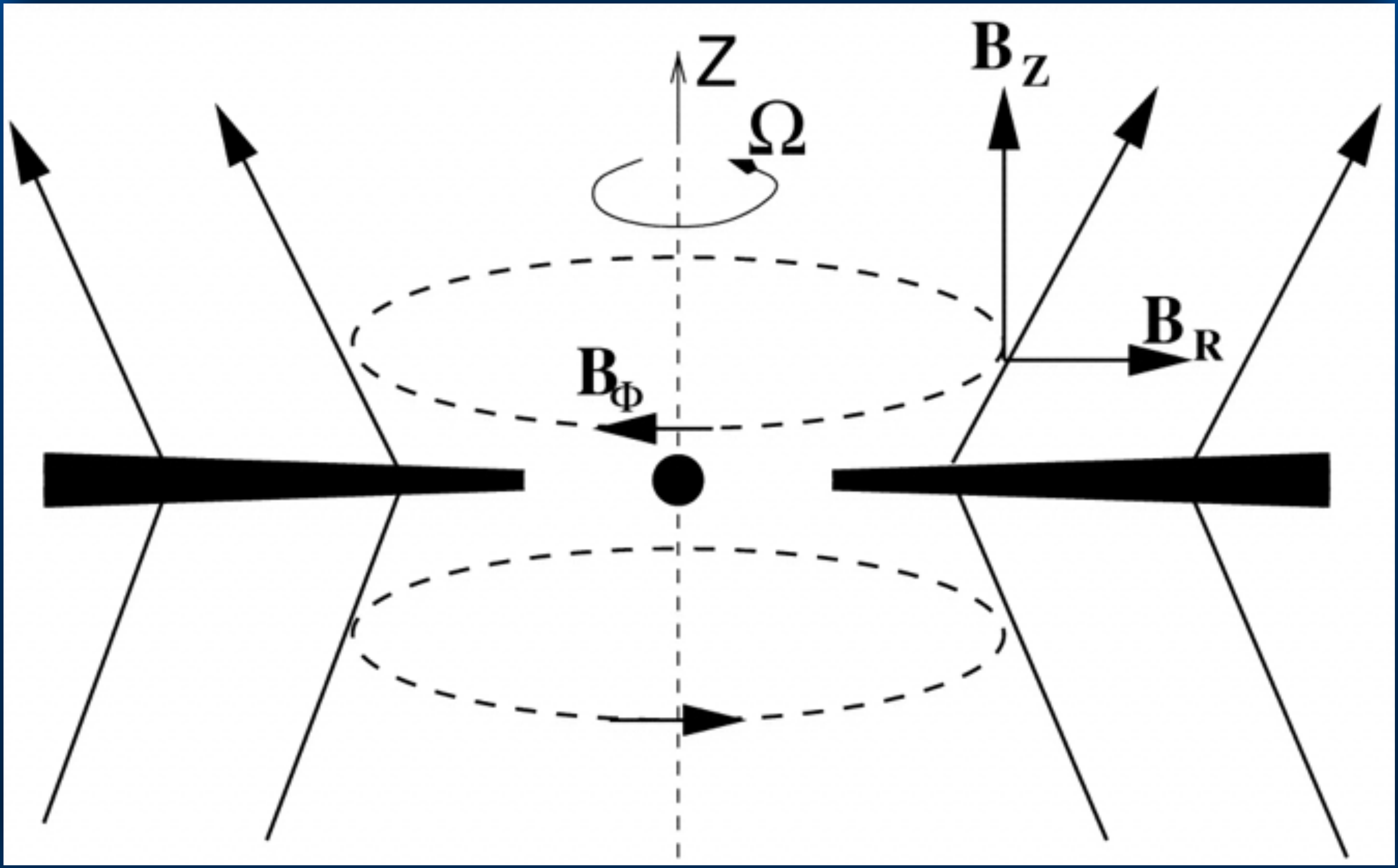

The effective potential per unit mass is the sum of the gravitational potential and a centrifugal term,

$$\Phi_{\mathrm{eff}} = -\frac{GM_{\mathrm{BH}}}{\sqrt{r^2+z^2}} - \frac{1}{2}\Omega_{\mathrm{m}}^2 r^2 .$$

In a Keplerian disk with magnetic field lines anchored at r_0

$$\Phi_{\mathrm{eff}} = -GM_{\mathrm{BH}}\left[\frac{r_0}{\sqrt{r^2+z^2}} + \frac{1}{2}\left(\frac{r}{r_0}\right)^2\right].$$

For a particle at on the disk surface to be in unstable equilibrium with respect to a small displacement along the field line, we must demand that the second derivative of the effective potential along the field line at (r_0, 0) is negative.

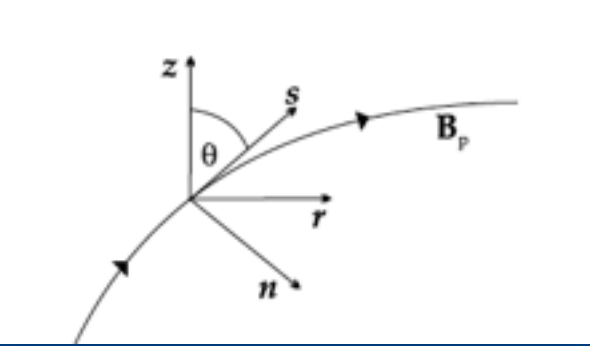

$$\frac{\partial^2 \Phi_{\mathrm{eff}}}{\partial s^2}(r_0, 0) = -\frac{G M_{\mathrm{BH}}}{r_0^3}\left(3 \sin\theta^2 - \cos\theta^2\right) < 0,$$

The condition for unstable equilibrium is then that $\theta > 30^\circ$; this is the minimum inclination the field lines must have in order to accelerate matter outwards from the surface of the disk

Magnetic acceleration

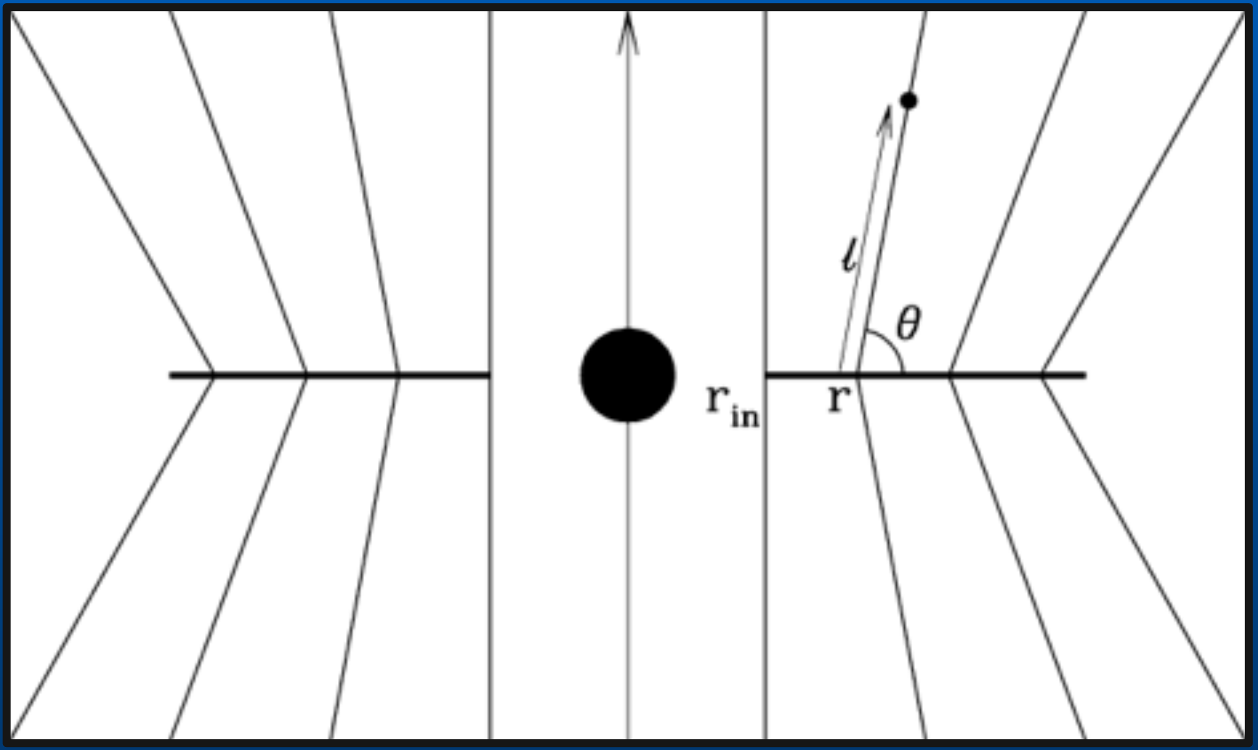

Efficient magneto-centrifugal acceleration:
Theta 90-theta>30 deg (Blandford & Payne 1982)

Magnetic acceleration

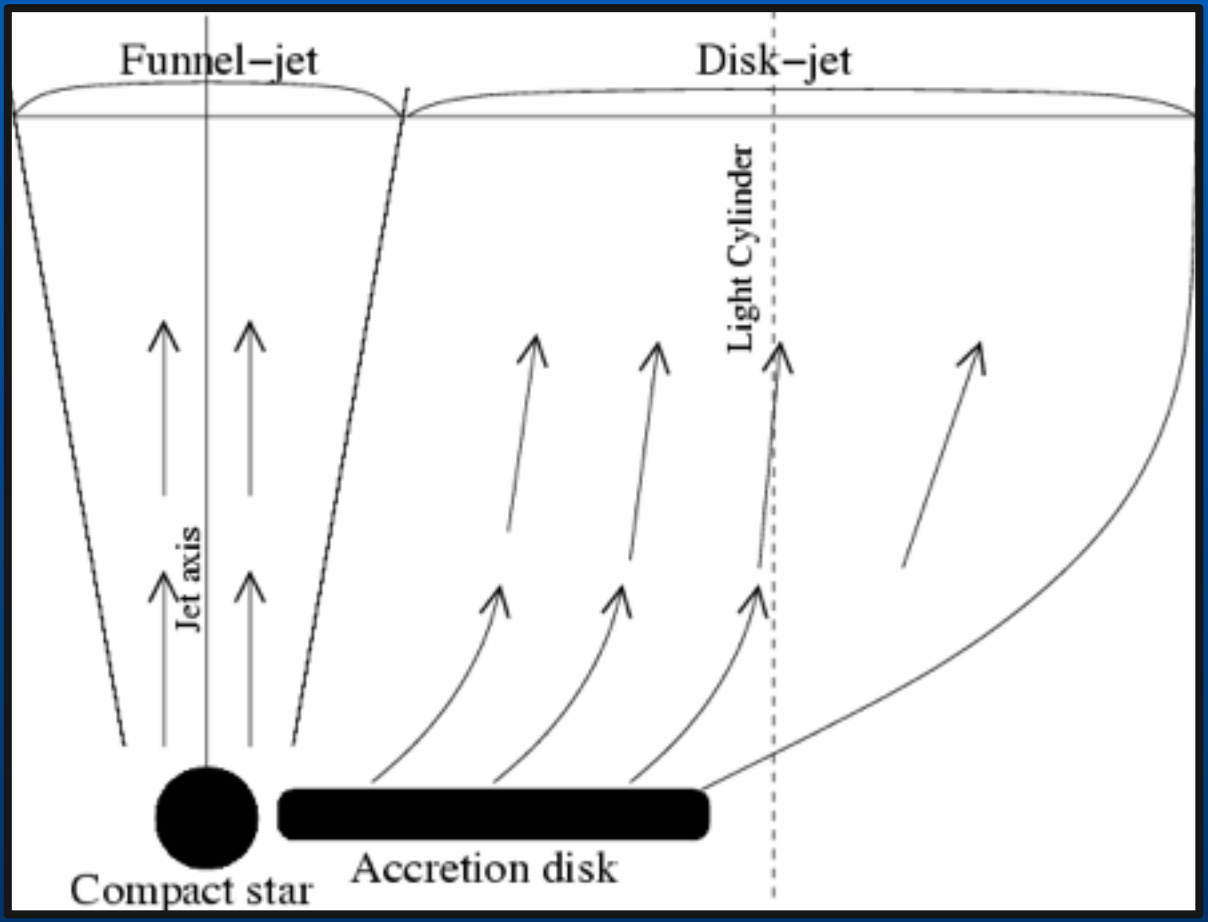

Magnetic towers

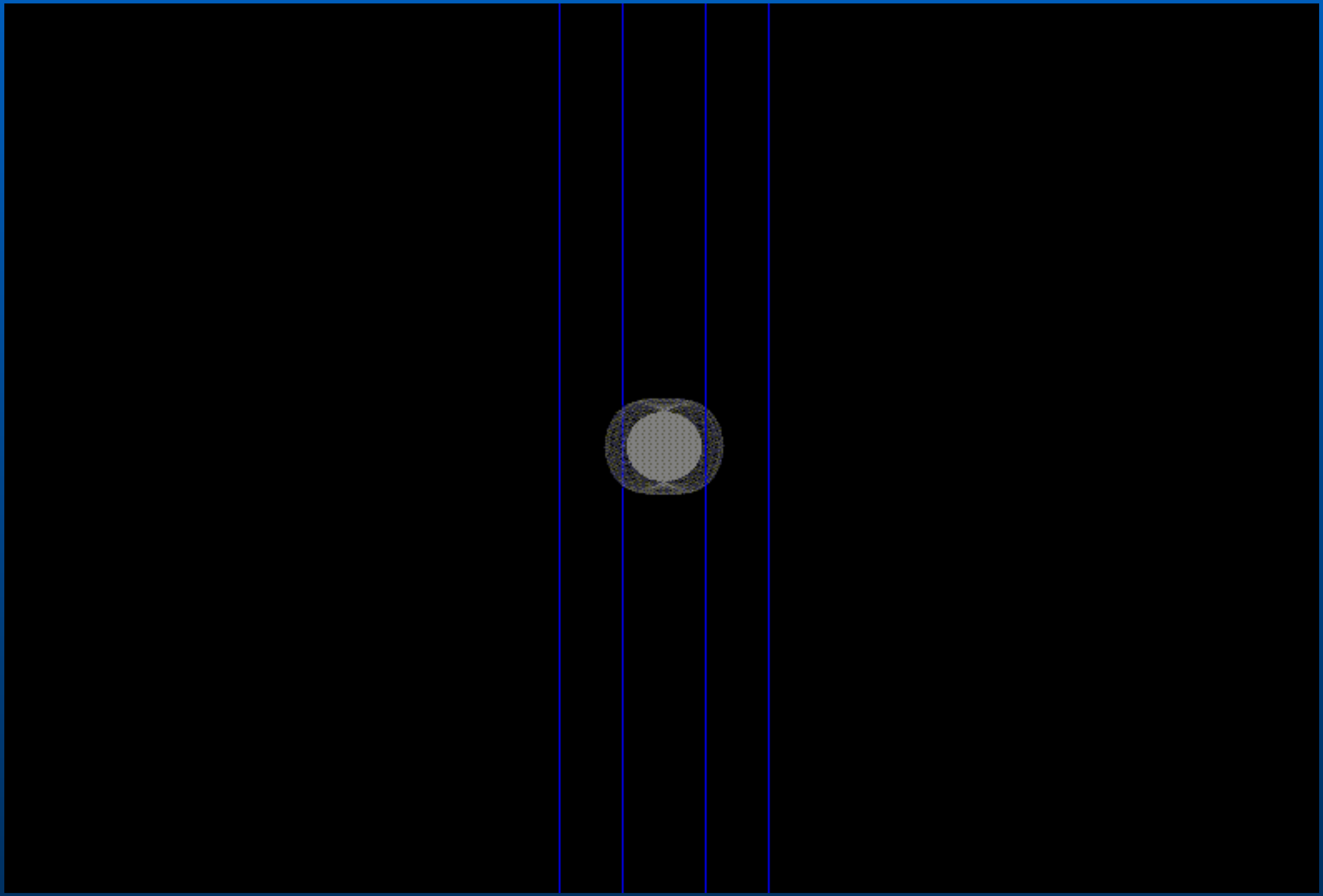

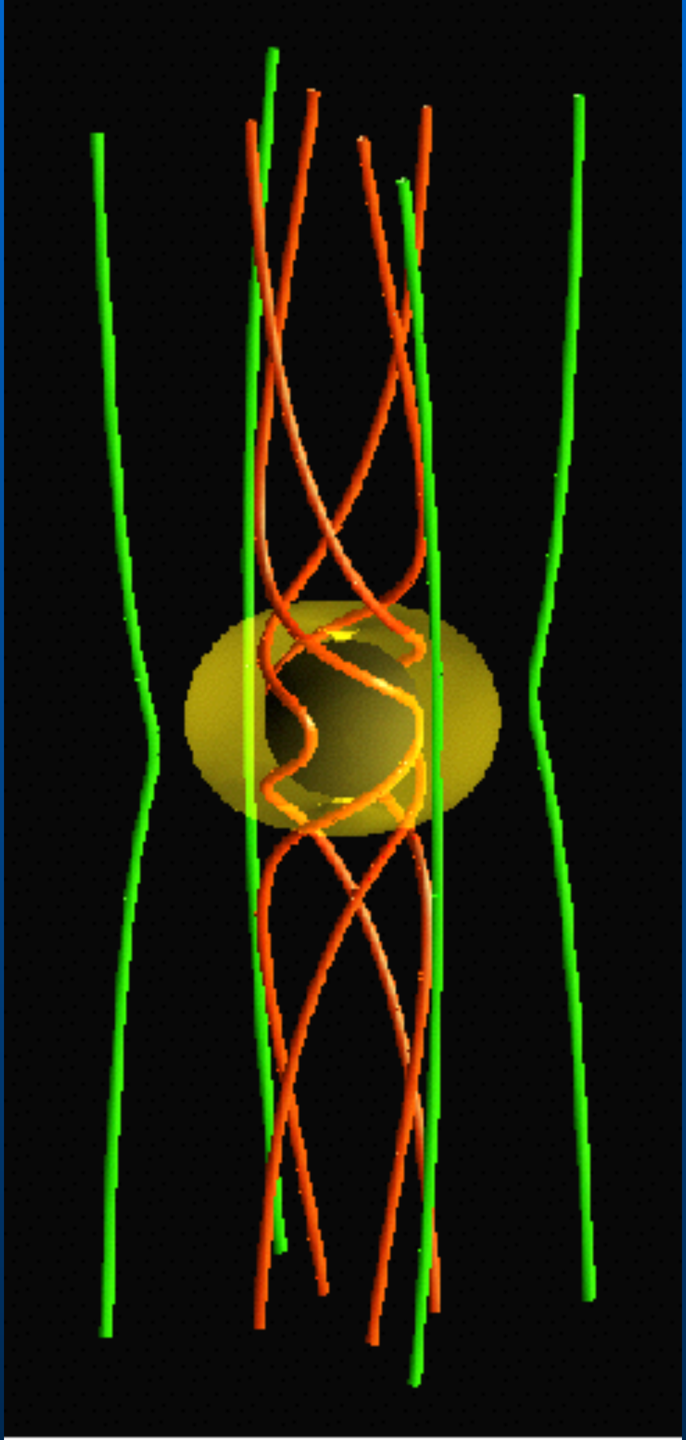

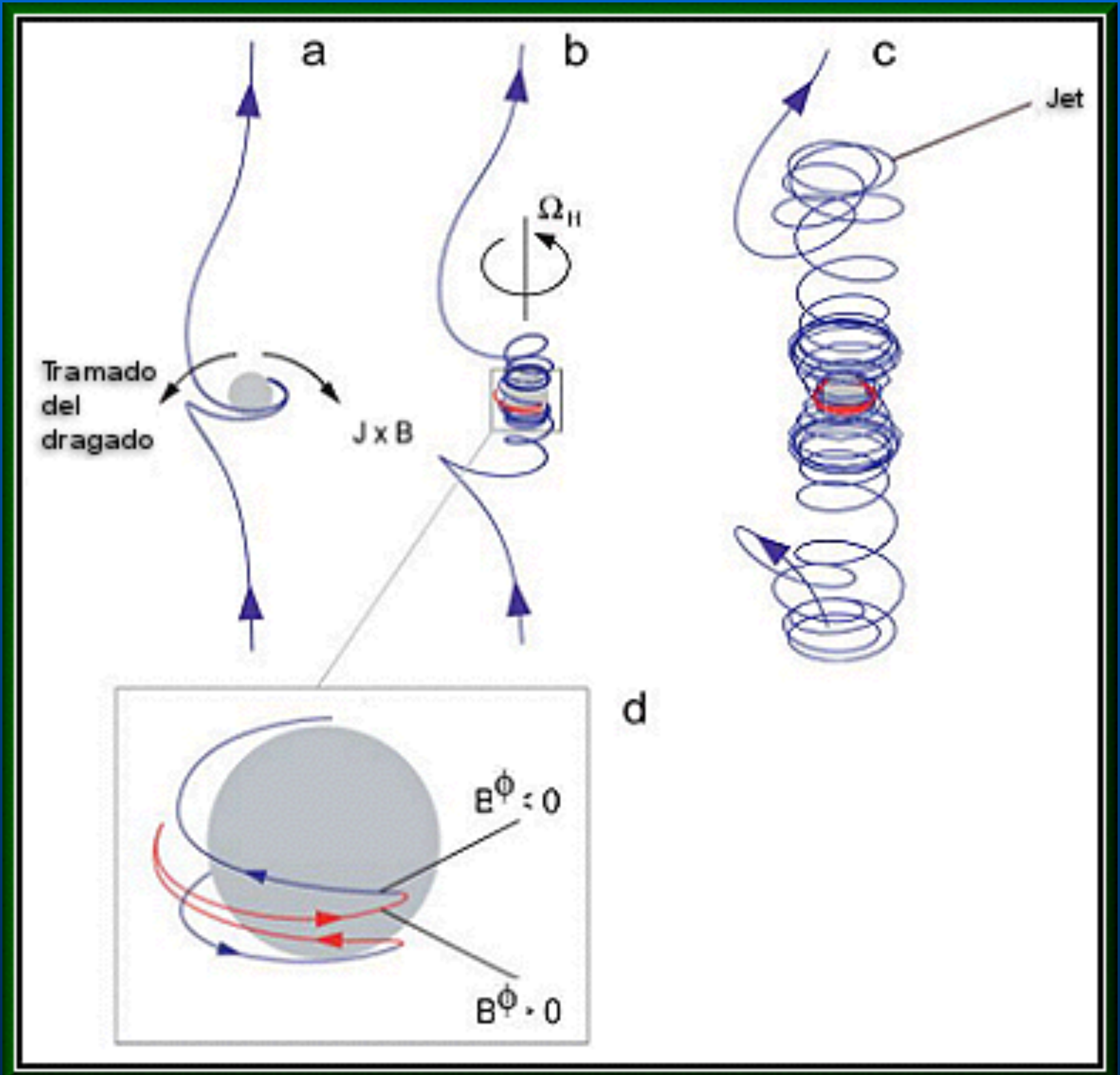

a
b
c
d
Tramado
del
dragado
J x B
Ω_H
Jet
$B^{\phi} < 0$
$B^{\phi} > 0$

Magnetic towers

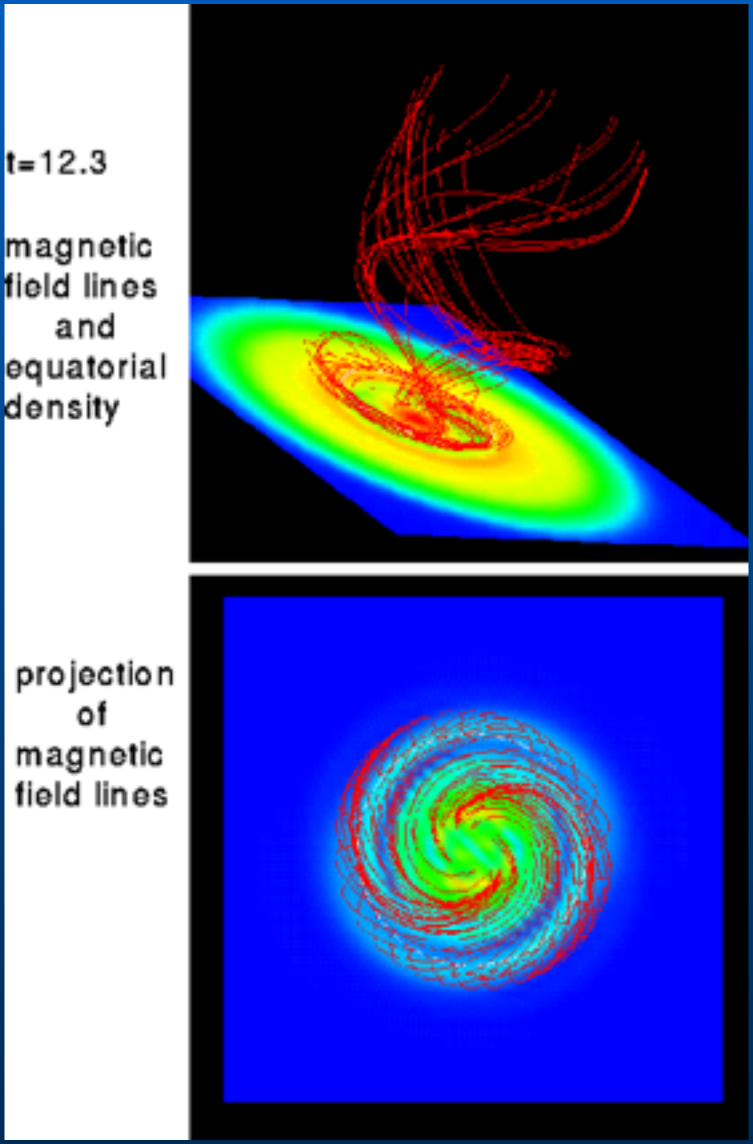

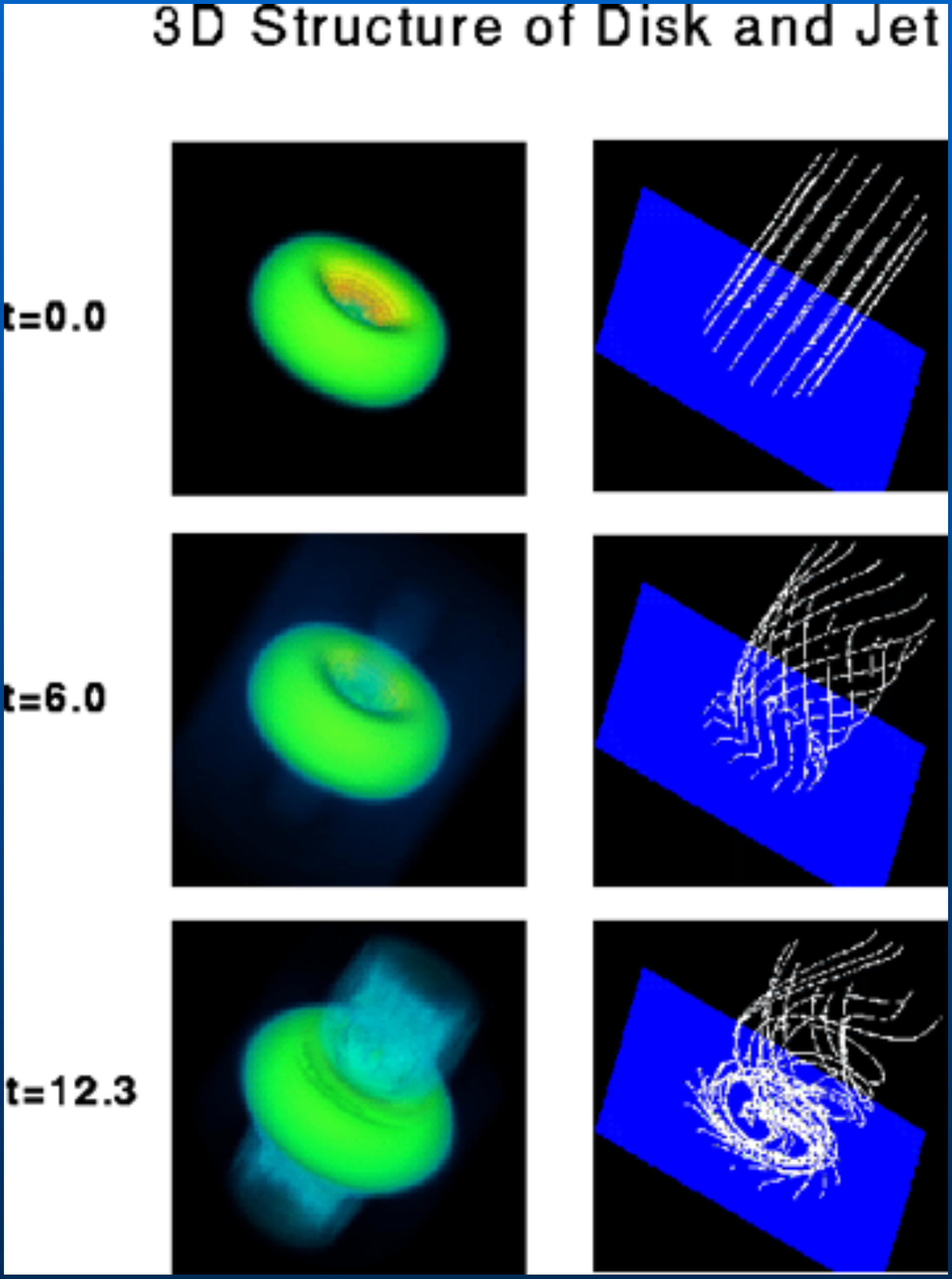
3D Structure of Disk and Jet
t=0.0
t=6.0
t=12.3

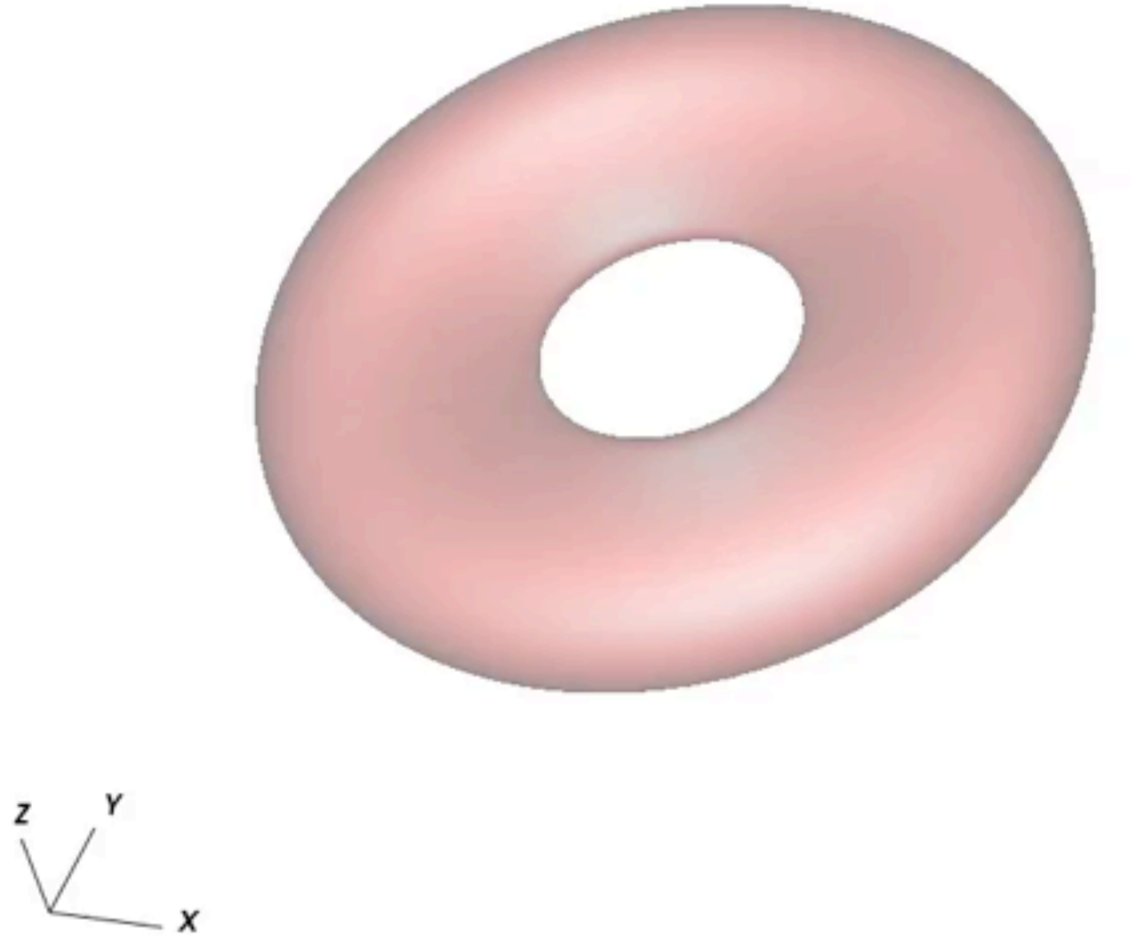
Z
Y
X

Blandford-Znajek mechanism

$$J_\mu F^{\mu\nu} = 0,$$

Force-free condition

$$F^{\mu\nu}_{;\nu} = \frac{4\pi}{c} J^\mu.$$

Maxwell equations in Kerr spacetime

$$L = \frac{G^2}{c^3} f(x) \frac{\omega(\Omega_\mathrm{H} - \omega)}{\Omega_\mathrm{H}^2} B_\mathrm{n}^2 M^2 a_*^2,$$

$$x = a/cr_\mathrm{h},$$

$$\Omega_\mathrm{H} \equiv \frac{a}{r_\mathrm{h}^2 + a^2/c^2}$$

$$f(x) = \frac{1+x^2}{x^2}\left[\left(x + \frac{1}{x}\right)\arctan x - 1\right],$$

Blandford-Znajek mechanism

$f \sim 1$ in the allowed range $0 \leq x \leq 1$.

$\omega = \Omega_{\rm H}/2$

$$L \approx 10^{46} \left(\frac{B_{\rm n}}{10^4\ {\rm G}} \right)^2 \left(\frac{M}{10^9 M_\odot} \right)^2 a_*^2\ {\rm erg\,s^{-1}}.$$

Different mechanisms for jet launching:

- Disk (Blandford & Payne 1982)
- BH (Blanford & Znajeck 1977)
- Ergosphere (Punsly & Coronity 1990)
- Magnetic towers (Kato et al 2004)

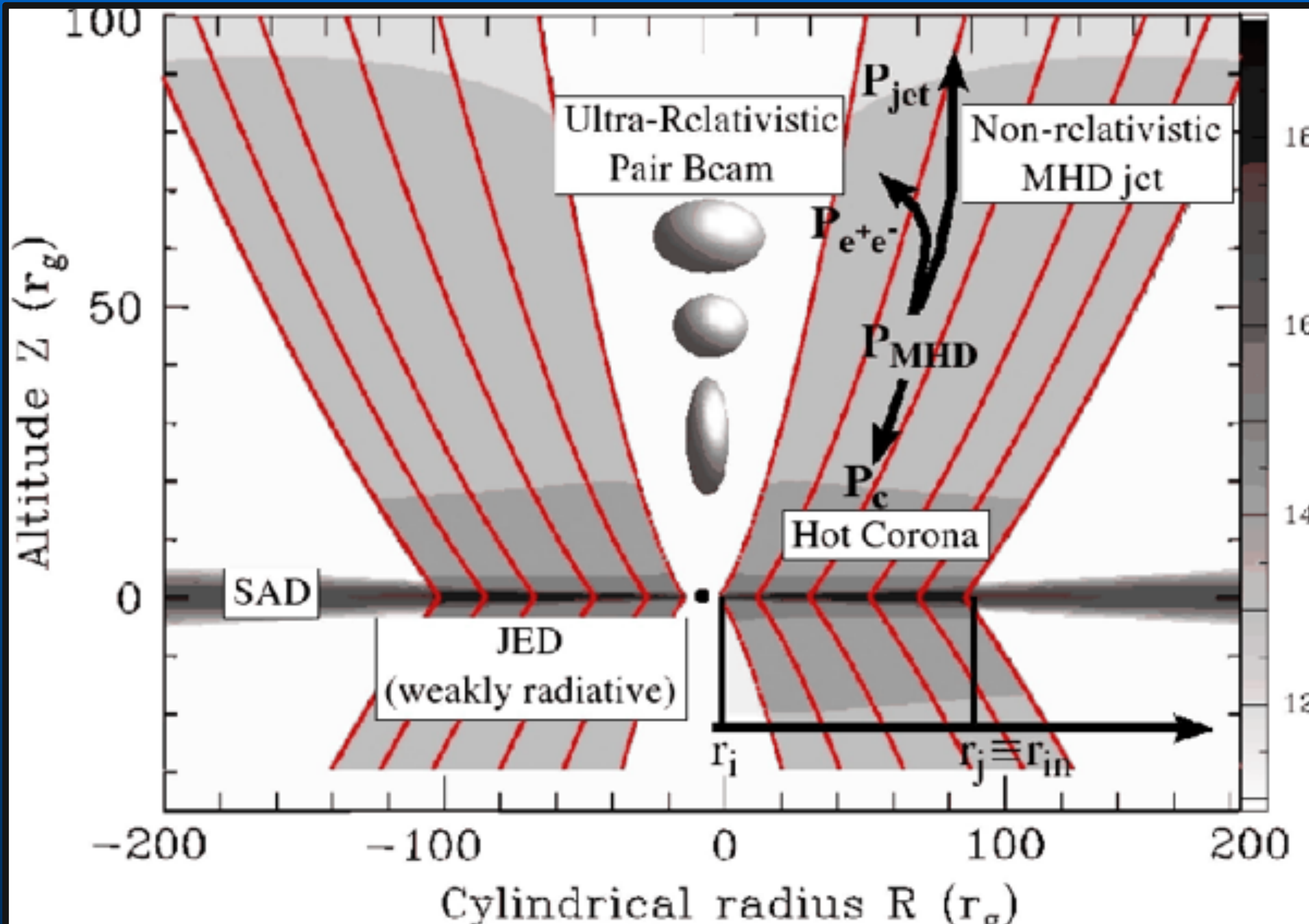

Ultra-Relativistic
Pair Beam
P_{jet}
Non-relativistic
MHD jet
$P_{e^+e^-}$
P_{MHD}
P_c
Hot Corona
SAD
JED
(weakly radiative)
r_i
$r_j \equiv r_{in}$
Altitude Z (r_g)
Cylindrical radius R (r_g)
100
50
0
−200
−100
0
100
200
12
14
16
18

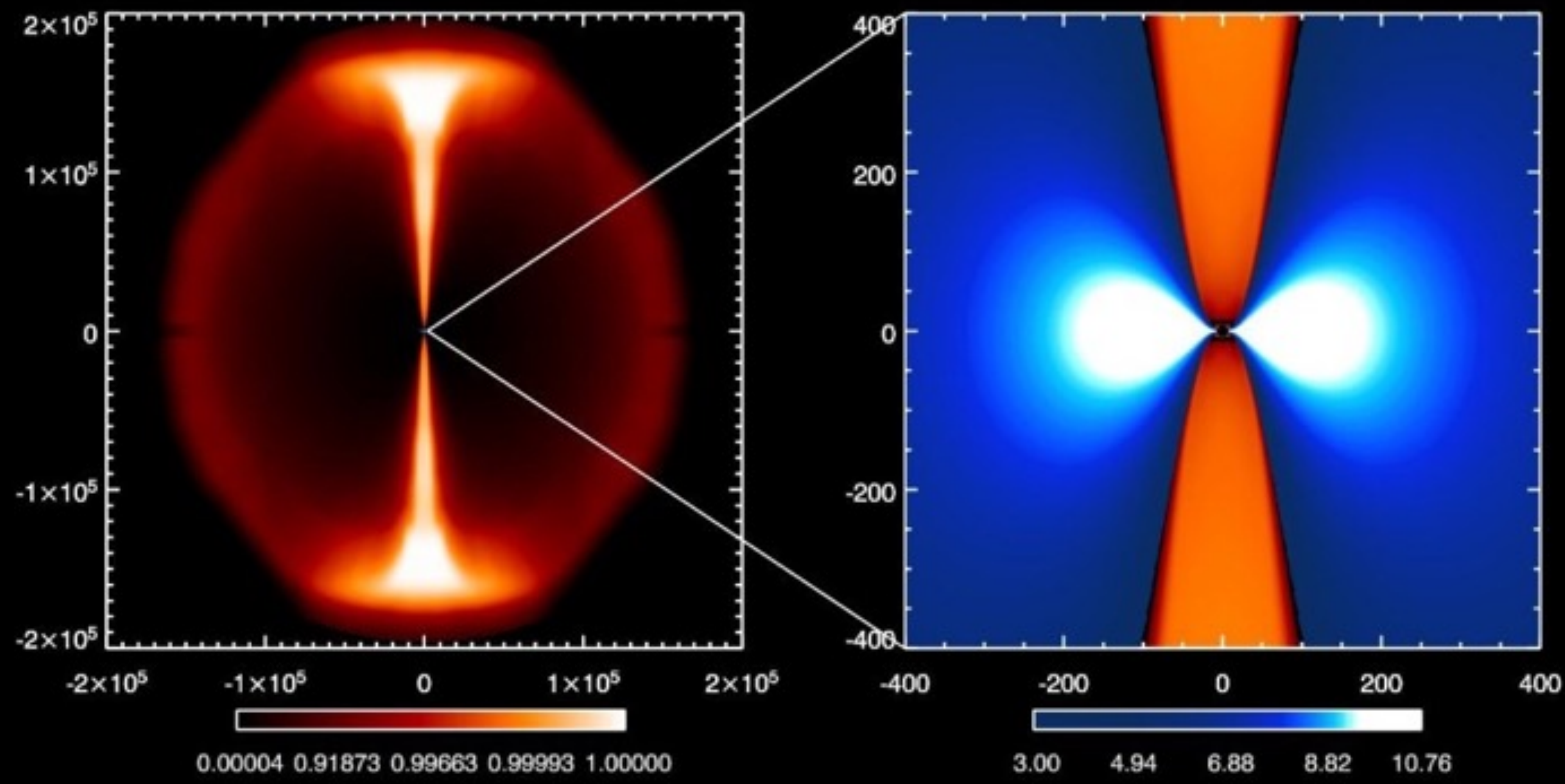

2×10^5
1×10^5
0
-1×10^5
-2×10^5
-2×10^5 -1×10^5 0 1×10^5 2×10^5
0.00004 0.91873 0.99663 0.99993 1.00000
400
200
0
-200
-400
-400 -200 0 200 400
3.00 4.94 6.88 8.82 10.76

Relativistic Jets From Collapsars

S.E. Woosley's Group

Inital Model: he15

480 radial zones, 200 angular zones

Energy Deposition Rate: 10^{51} ergs/s

Half Opening Angle: 20

$f_e(E_{th}/E_{tot})$: 0.67

Lorentz Factor: 50

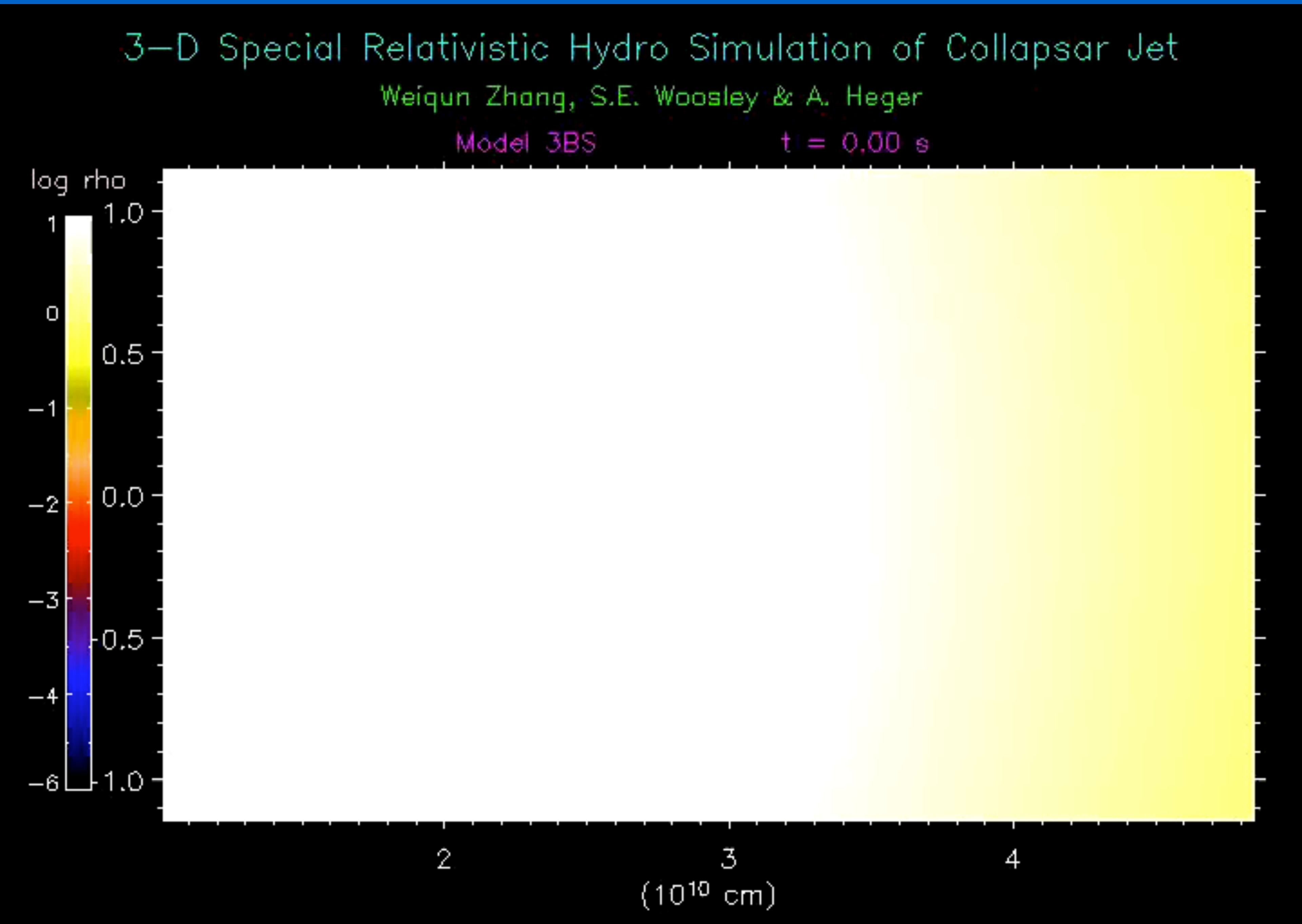
3-D Special Relativistic Hydro Simulation of Collapsar Jet
Weiqun Zhang, S.E. Woosley & A. Heger
Model 3BS
t = 0.00 s
log rho
1
0
-1
-2
-3
-4
-6
1.0
0.5
0.0
-0.5
-1.0
2
3
4
(10^10 cm)

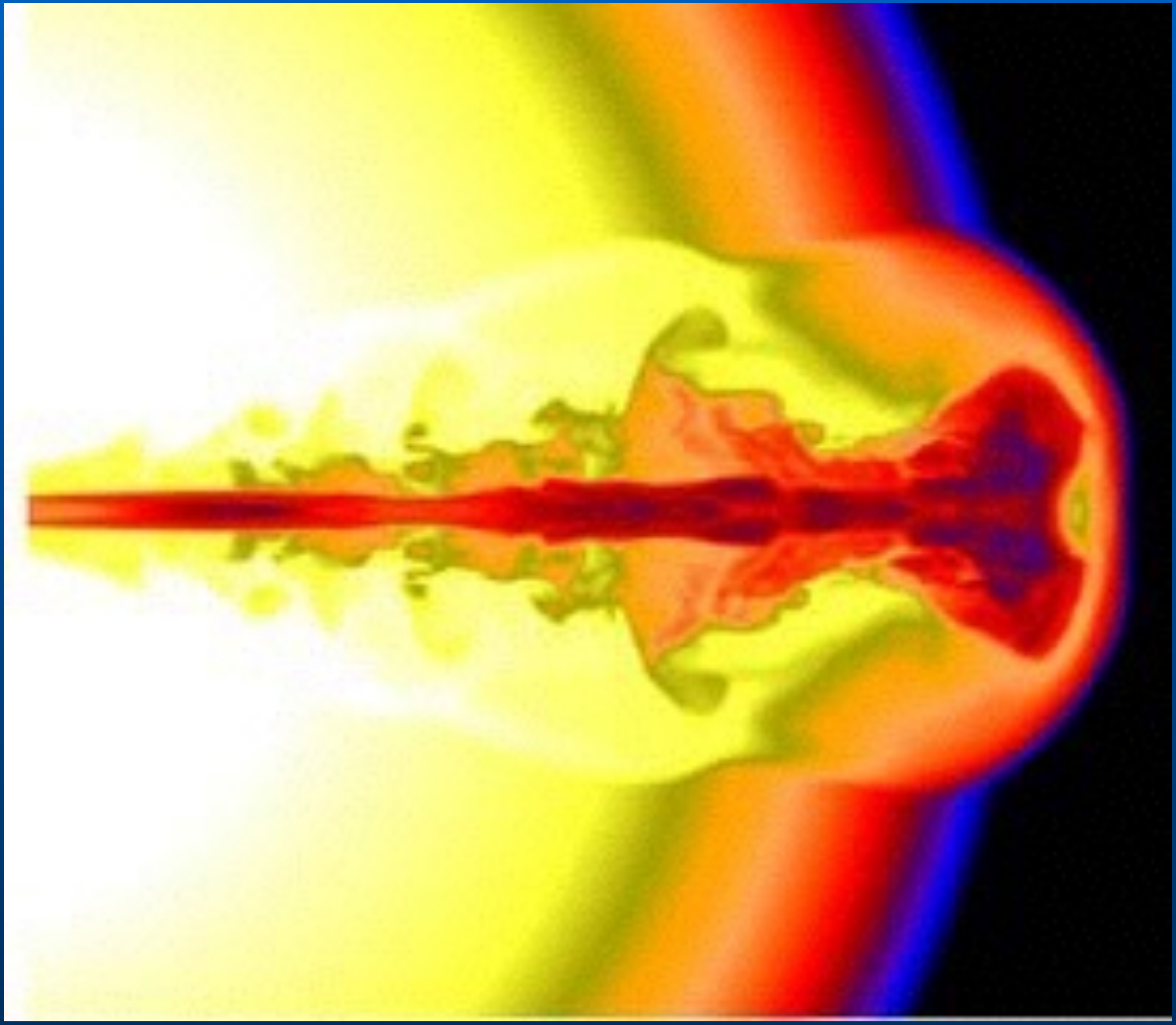

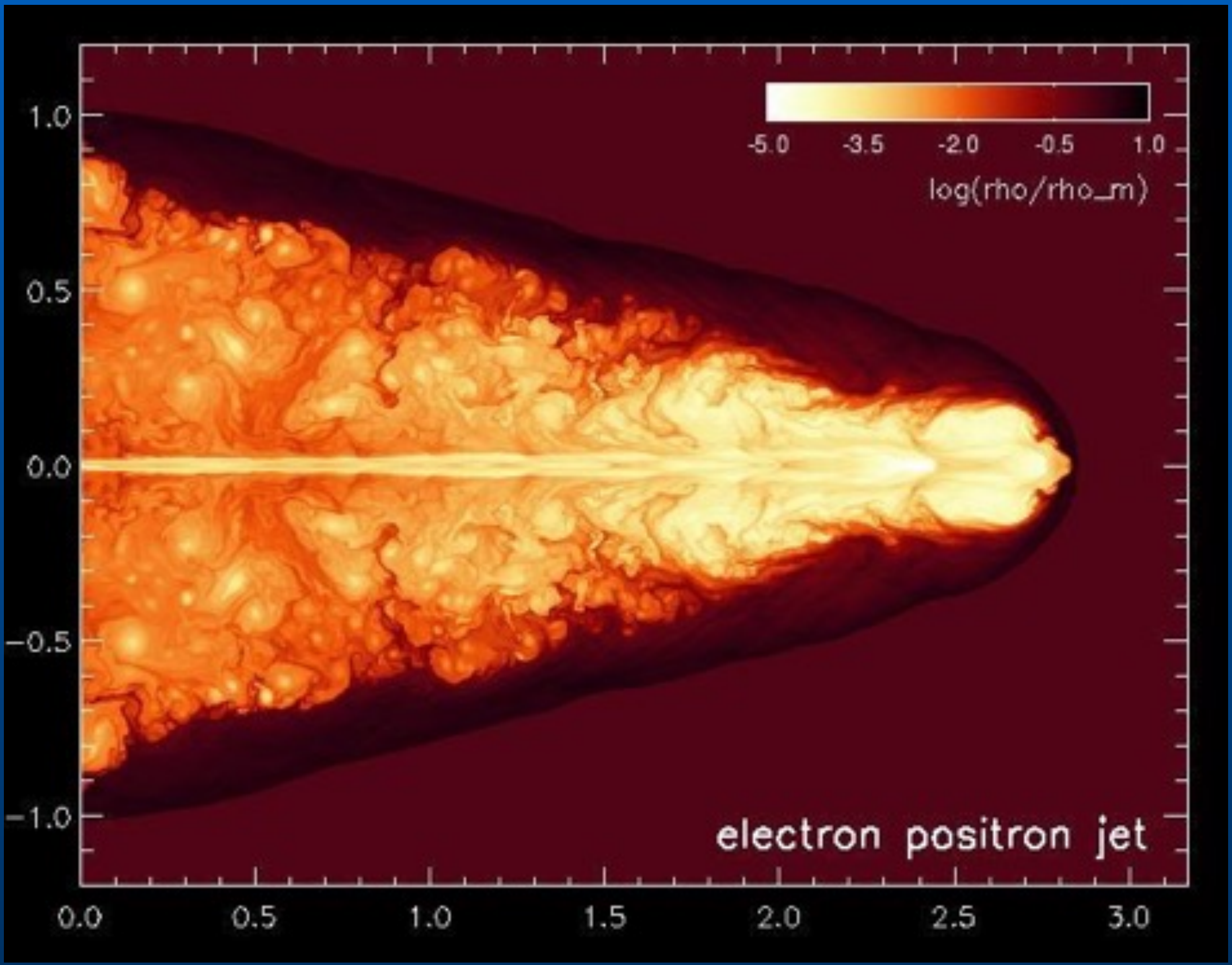

1.0
0.5
0.0
−0.5
−1.0
0.0
0.5
1.0
1.5
2.0
2.5
3.0
-5.0
-3.5
-2.0
-0.5
1.0
log(rho/rho_m)
electron positron jet

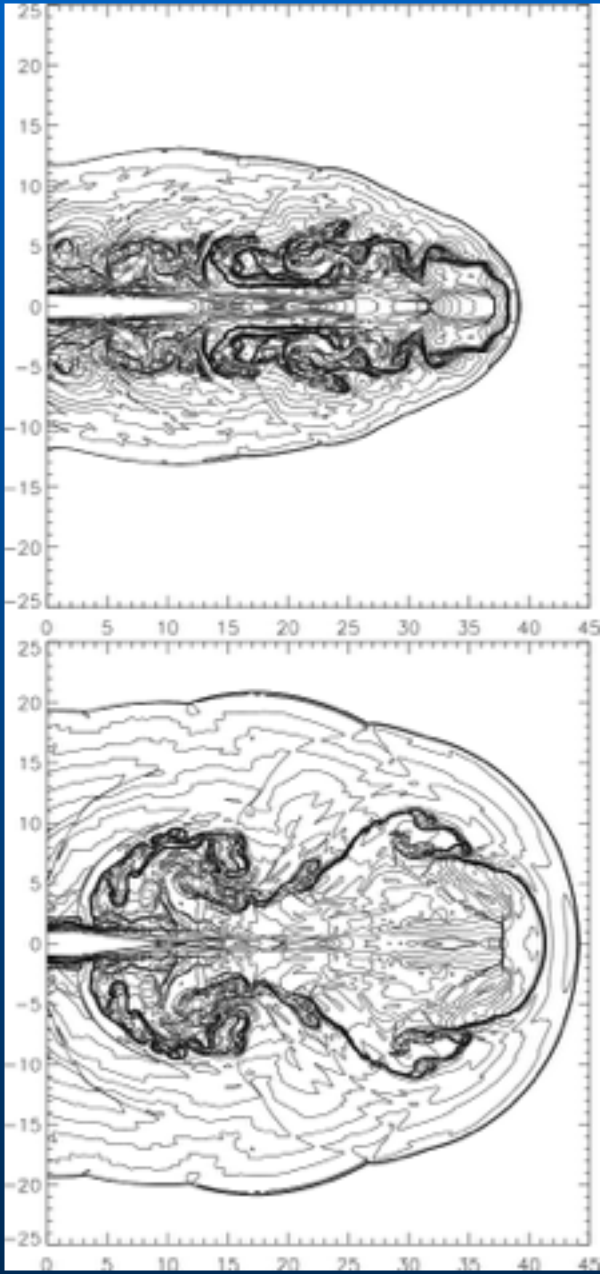

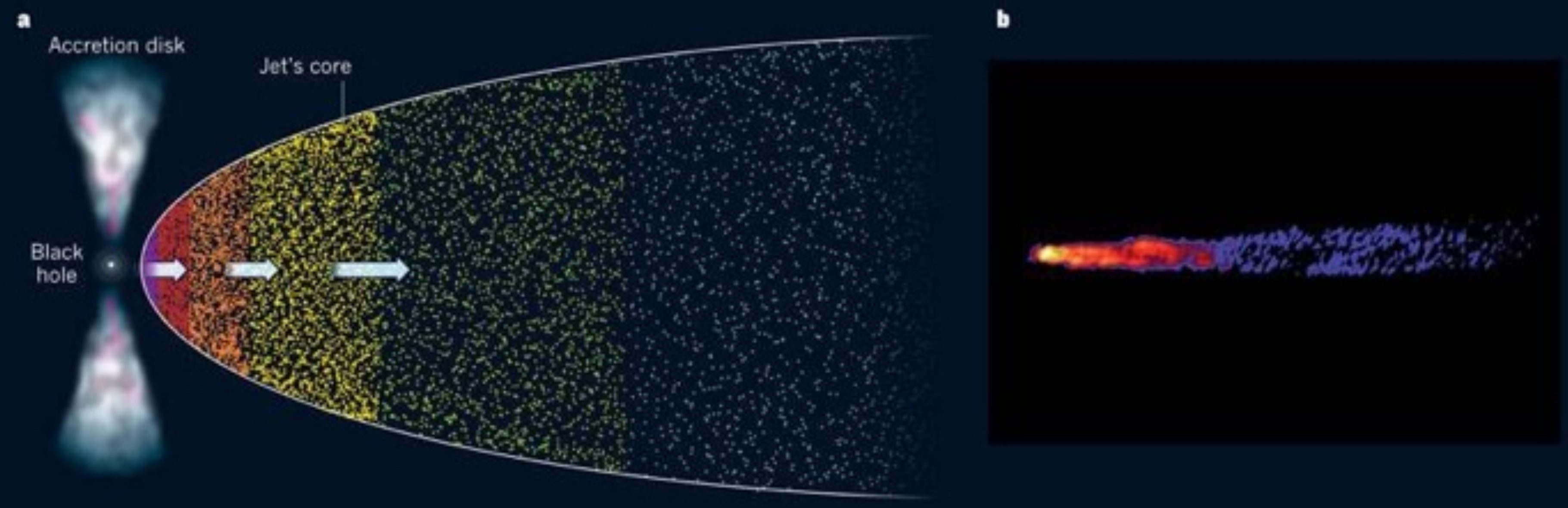
a
Accretion disk
Jet's core
Black
hole
b

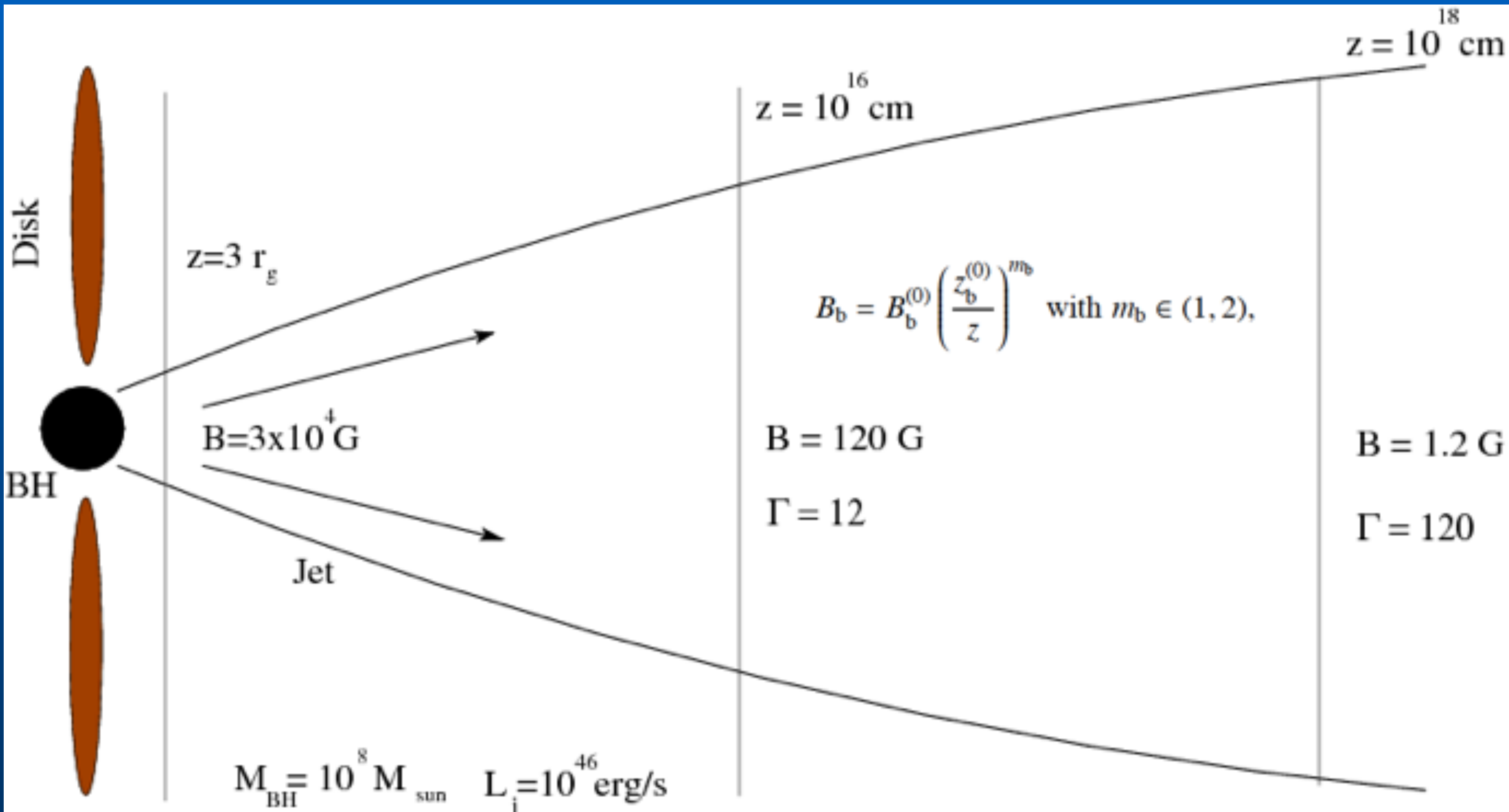
Disk
BH
z=3 r$_g$
B=3x10^{4}G
Jet
M_{BH}= 10^8 M $_{sun}$ L_j=10^{46}erg/s
z = 10^{16} cm
$B_b = B_b^{(0)} \left(\frac{z_b^{(0)}}{z} \right)^{m_b}$ with $m_b \in (1, 2)$,
B = 120 G
Γ = 12
z = 10^{18} cm
B = 1.2 G
Γ = 120

The "lepto/hadronic" jet model (in a nutshell)

- Physical conditions near the jet base are similar to those of the corona (e.g. Reynoso et al. 2011; Romero & Vila 2008, 2009; Vila & Romero 2010, Vila et al. 2012, Reynoso et al. 2012, Romero et al. 2010, 2014; Vieyro & Romero 2012, Pepe et al. 2015) .
- The jet launching region is quite close to the central compact object (few R_g)
- Hot thermal plasma is injected at the base, magnetically dominated jet to start with.
- Jet plasma accelerates longitudinally due to pressure gradients, expands laterally with sound speed (Bosch-Ramon et al. 2006)
- The plasma cools as it moves outward along the jet. As the plasma accelerates the local magnetic field decreases.

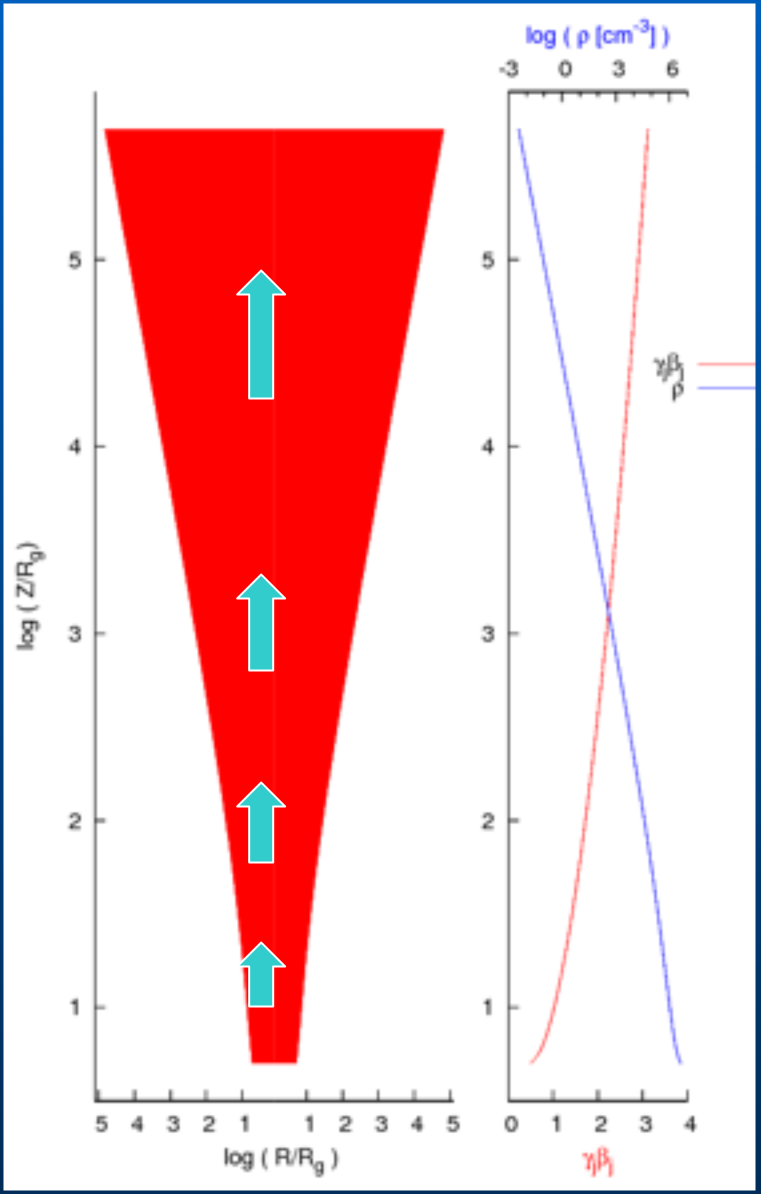

Maitra et al. (2009)

Jet Model – 1. Structure

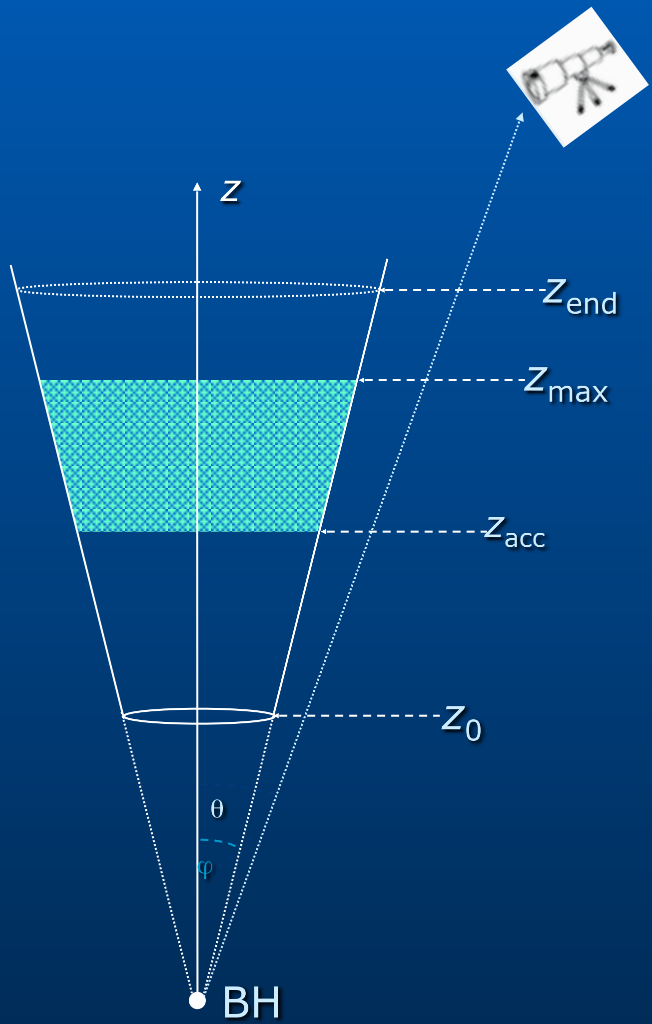

- z_0 : base of the jet; ~50 R_g
- $z_{acc} < z < z_{max}$: acceleration region; injection of relativistic particles.
- z_{end} : "end" of the radiative jet
- φ : jet opening angle
- θ : viewing angle; moderate

Jet Model – 2. Power

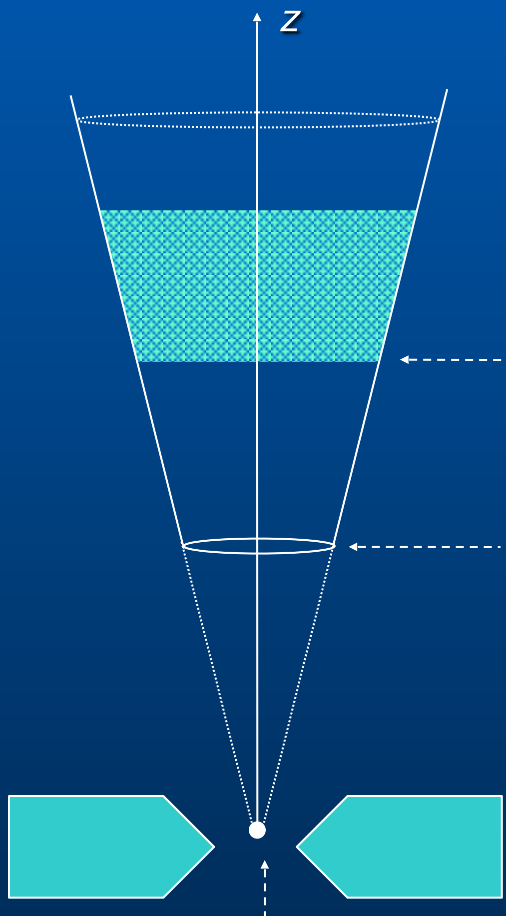

$$L_{rel} = q_{rel} L_{jet}$$

$$L_{jet} = \frac{1}{2} q_{jet} L_{accr}$$

$$L_{accr} = q_d L_{Edd}$$

Content of relativistic particles…

$$L_{rel} = L_p + L_e \qquad L_p = a\, L_e$$

$$Q(E,z) \propto E^{-\alpha} \exp\left(-\frac{E}{E_{\max}} \right) f(z)$$

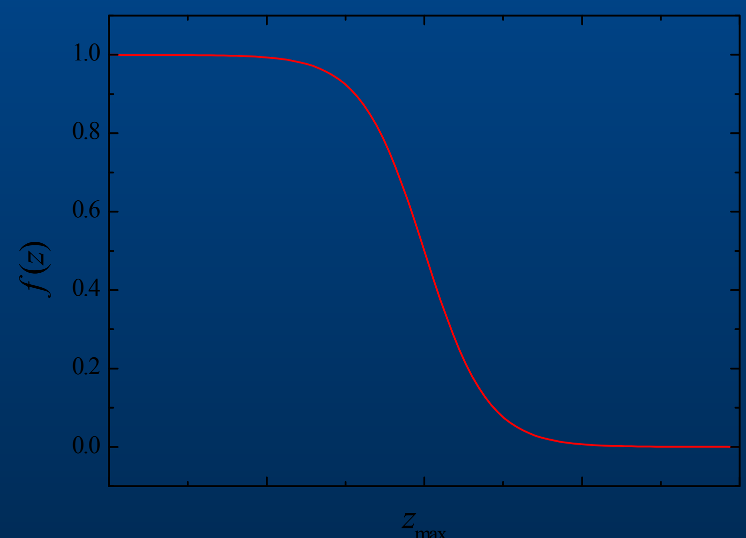

Jet Model – 3. Acceleration and losses

Maximum energy determined by balance of cooling and acceleration rates

- Acceleration: diffusive shock acceleration (only when the magneization goes below 1).

$$t_{acc}^{-1} = \eta ecB(z)E^{-1} \qquad \eta < 1$$

$$B(z) = B_0 \left(\frac{z_0}{z} \right)^{-m} \qquad 1 \leq m \leq 2$$

- Cooling processes: interaction with magnetic field, photon field and matter
  - Synchrotron
  - Relativistic Bremsstrahlung
  - Proton-proton collisions (pp)
  - Inverse Compton (over ALL photon fields)
  - Proton-photon collisions (pγ)
  - Adiabatic cooling

Jet Model – 4. Particle distributions

Calculation of particle distributions: injection, cooling, decay, and convection

$$\Gamma_{\rm jet}\frac{\partial N}{\partial t}+\frac{\partial[\Gamma_{\rm jet}v_{\rm conv}N]}{\partial z}+\frac{\partial}{\partial E}\left(\frac{dE}{dt}N\right)+\frac{N}{T_{\rm dec}}=Q(E,z).$$

Also for secondary particles: charged pions, muons and electron-positron pairs (see Reynoso & Romero 2009, Vila & Romero 2011, Reynoso et al. 2012).

- Direct pair production $p+\gamma\rightarrow p+e^{+}+e^{-}$ $\gamma+\gamma\rightarrow e^{+}+e^{-}$

- Photomeson production & pp collisions

$$\left.\begin{array}{l} p+p\rightarrow p+a\pi^{o}+b(\pi^{+}+\pi^{-}) \\ p+\gamma\rightarrow p+a\pi^{o}+b(\pi^{+}+\pi^{-}) \end{array}\right] \; \pi^{\pm}\rightarrow\mu^{\pm}+\nu_{\mu}\left(\bar{\nu}_{\mu}\right) \longrightarrow \mu^{\pm}\rightarrow e^{\pm}+\nu_{e}\left(\bar{\nu}_{e}\right)+\nu_{\mu}\left(\bar{\nu}_{\mu}\right)$$

Non-thermal radiative processes in jets

- Relativistic particles: electrons, protons, secondary particles ($\mu^{\pm}$, $\pi^{\pm}$, $e^{\pm}$)
- Target fields: magnetic fields, radiation fields, matter fields

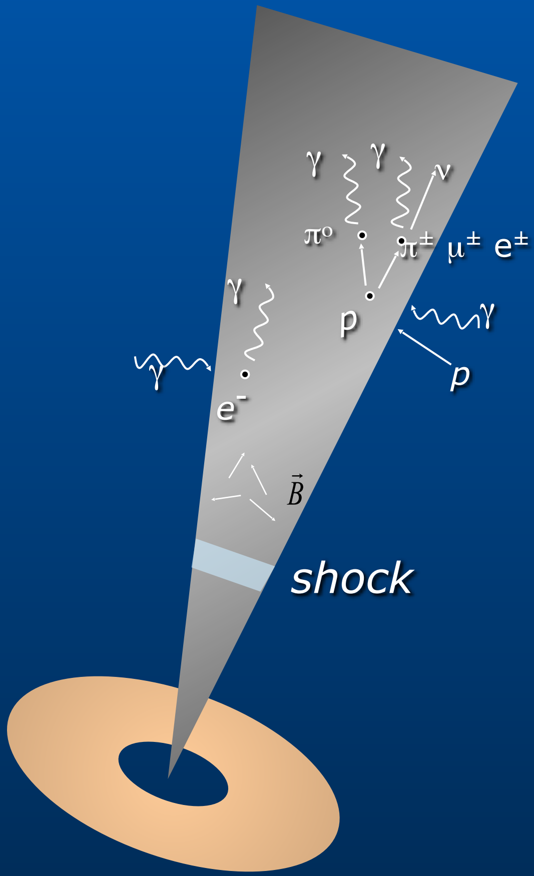

- Acceleration mechanism
  - Diffusive shock acceleration
  - Turbulent magnetic reconnection

$$Q(E) \propto E^{-\alpha}$$

- Target fields
  - Internal: locally generated photon fields, magnetic field, comoving matter field
  - External: depending on the context
    - stellar winds and photons,
    - accretion disc photons,
    - clumps, clouds, ISM…

Evolution of the bulk Lorentz factor of the jet

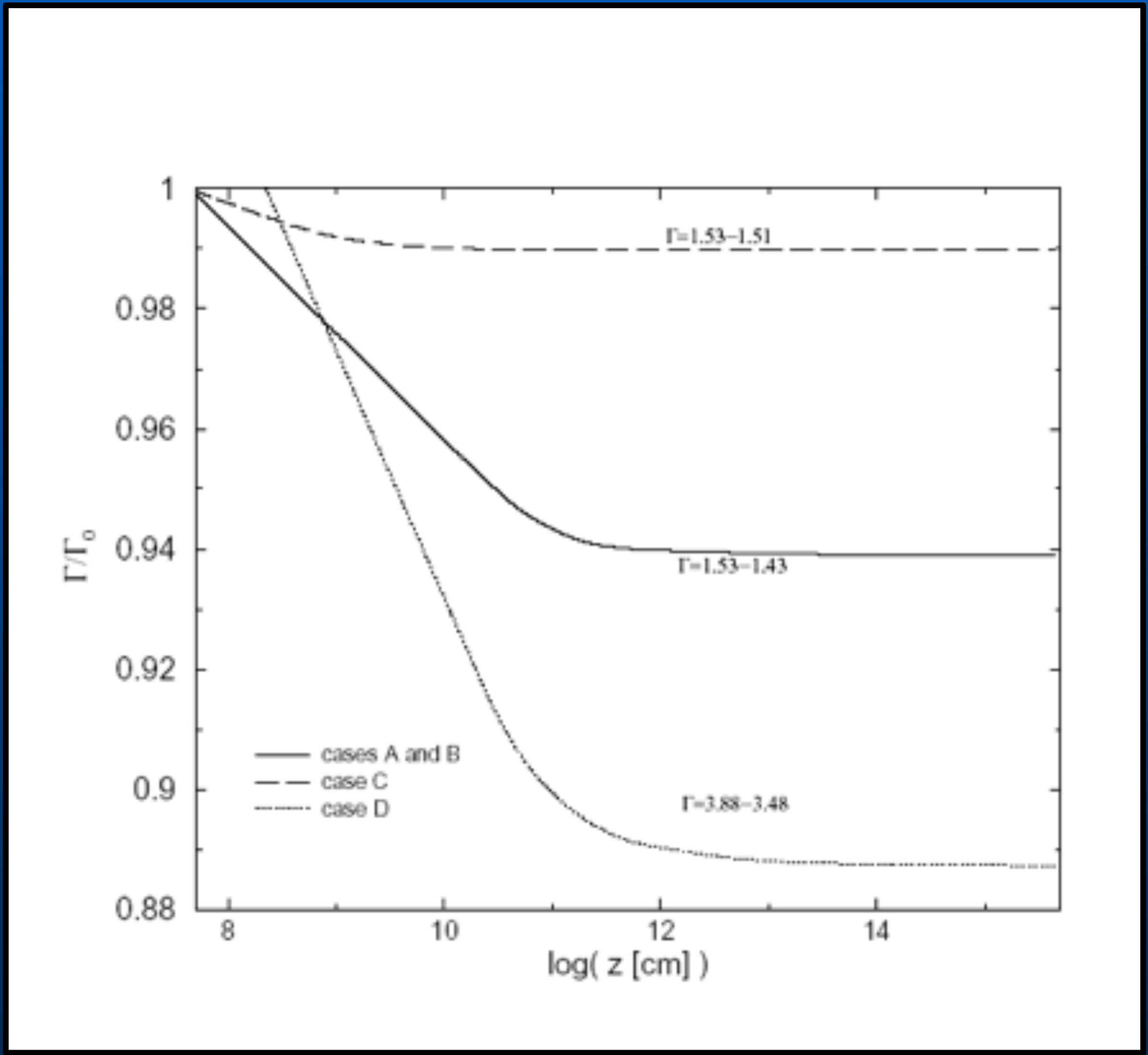

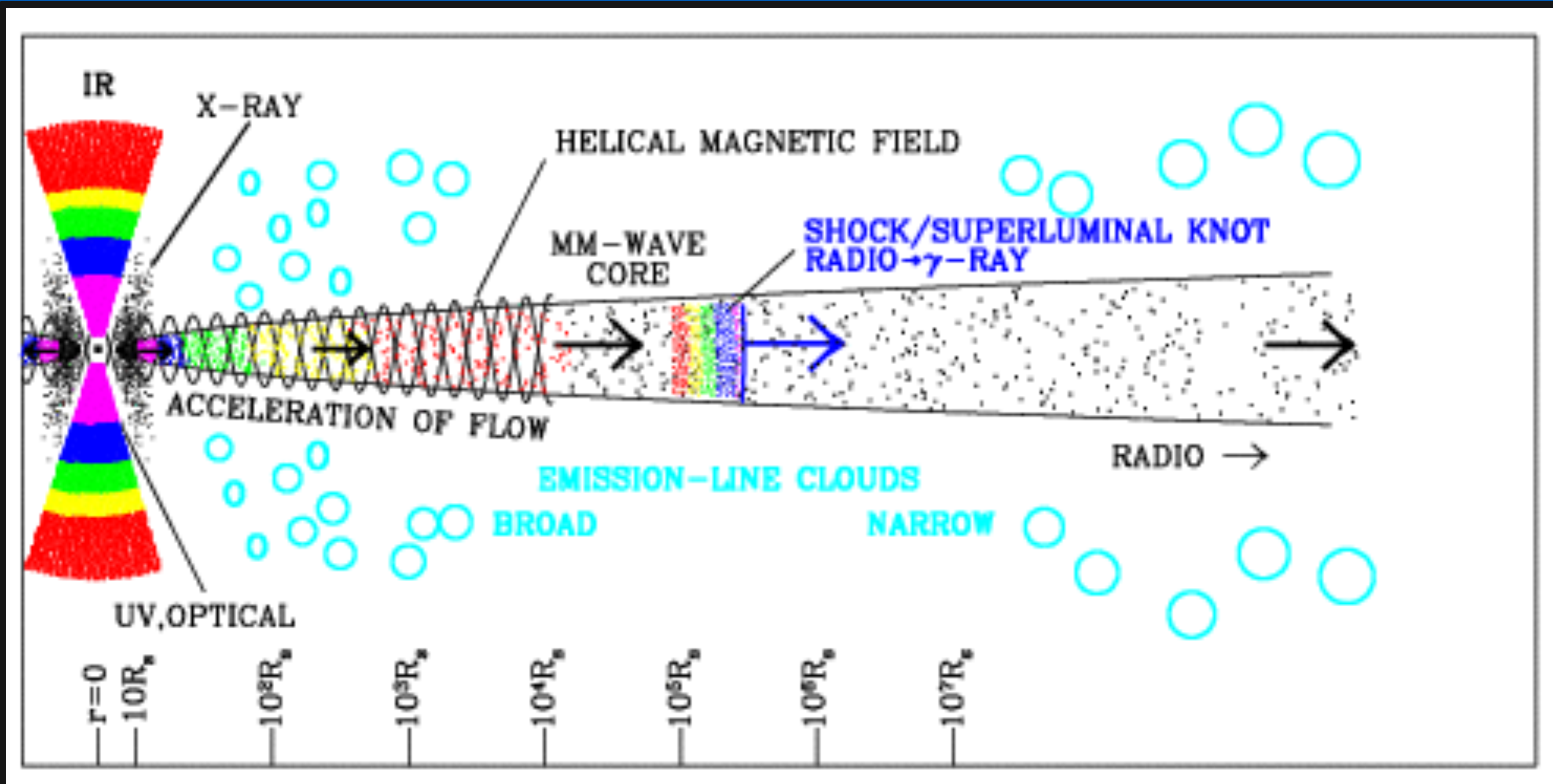

IR
X-RAY
HELICAL MAGNETIC FIELD
MM-WAVE
CORE
SHOCK/SUPERLUMINAL KNOT
RADIO→γ-RAY
ACCELERATION OF FLOW
RADIO →
EMISSION-LINE CLOUDS
BROAD
NARROW
UV,OPTICAL
r=0
10R_s
10^2R_s
10^3R_s
10^4R_s
10^5R_s
10^6R_s
10^7R_s

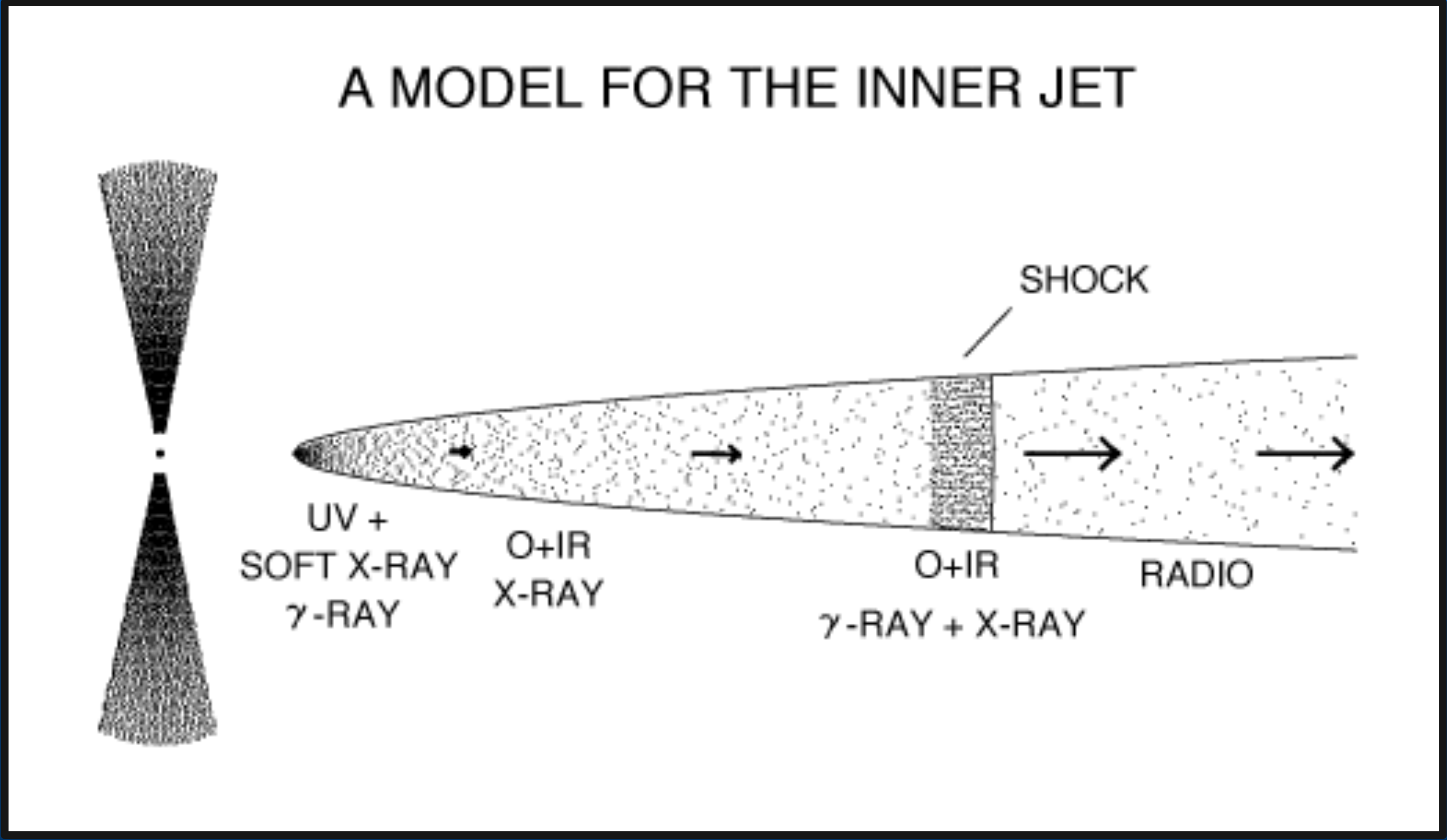
A MODEL FOR THE INNER JET
SHOCK
UV +
SOFT X-RAY
γ-RAY
O+IR
X-RAY
O+IR
γ-RAY + X-RAY
RADIO

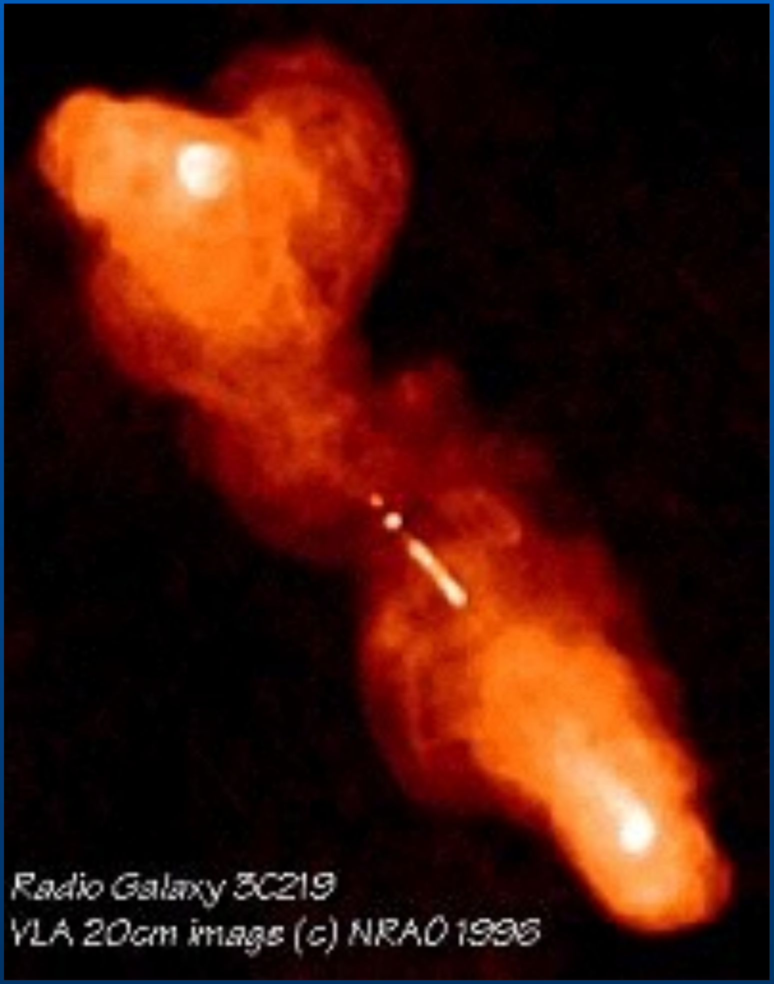
Radio Galaxy 3C219
VLA 20cm image (c) NRAO 1996

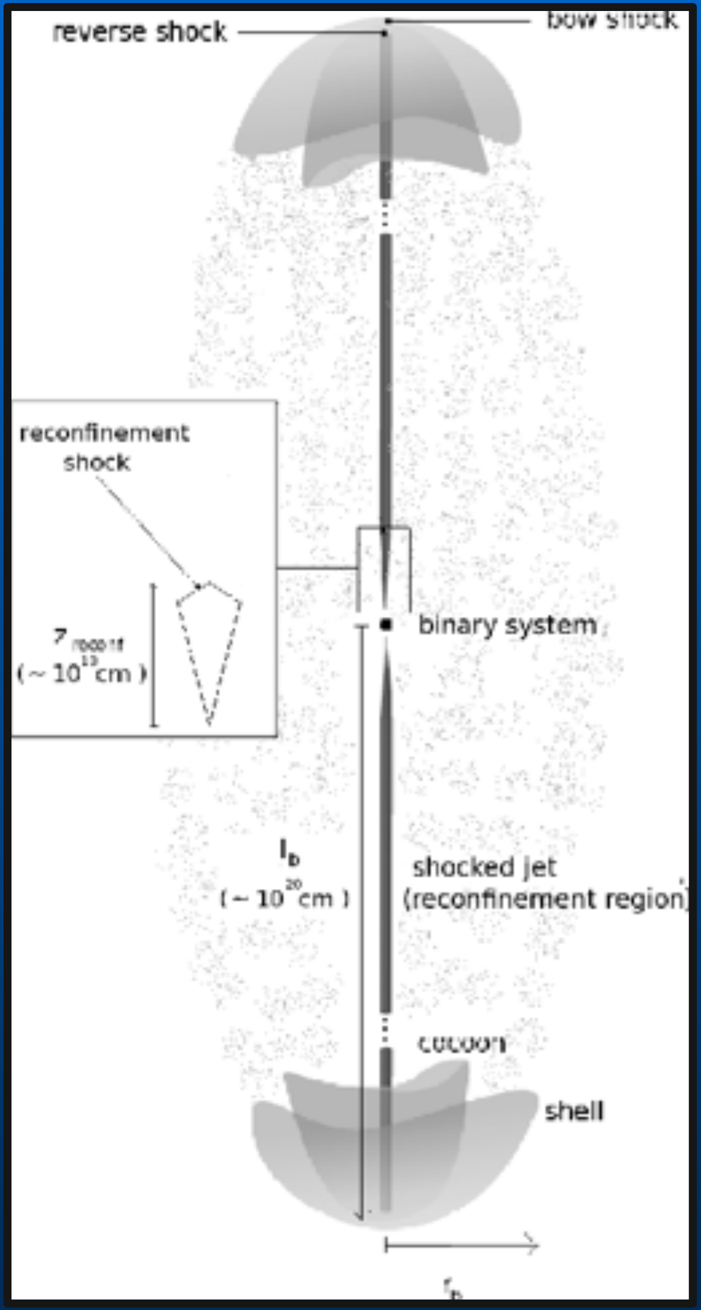
reverse shock
bow shock
reconfinement shock
binary system
shocked jet
(reconfinement region)
cocoon
shell

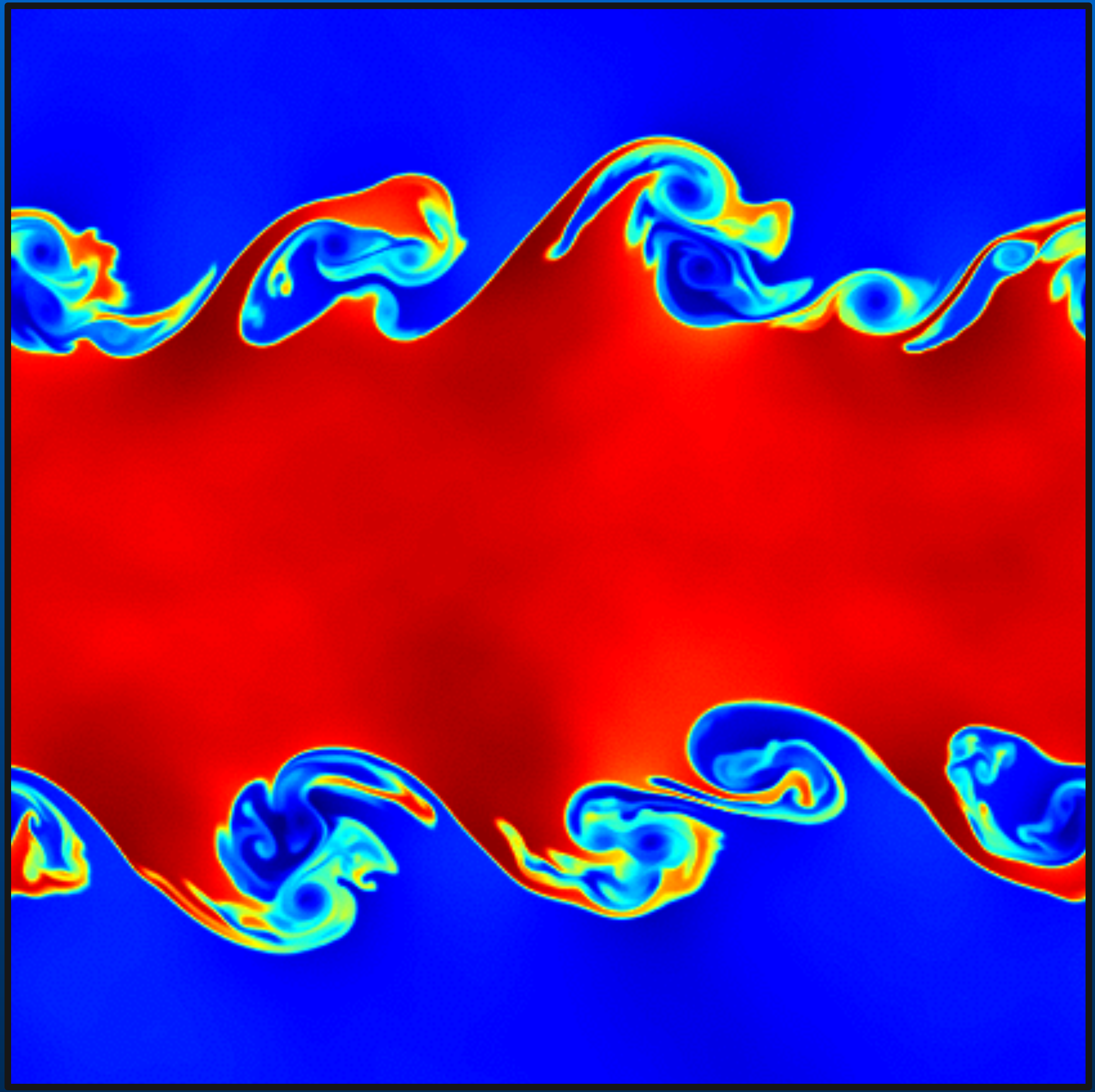

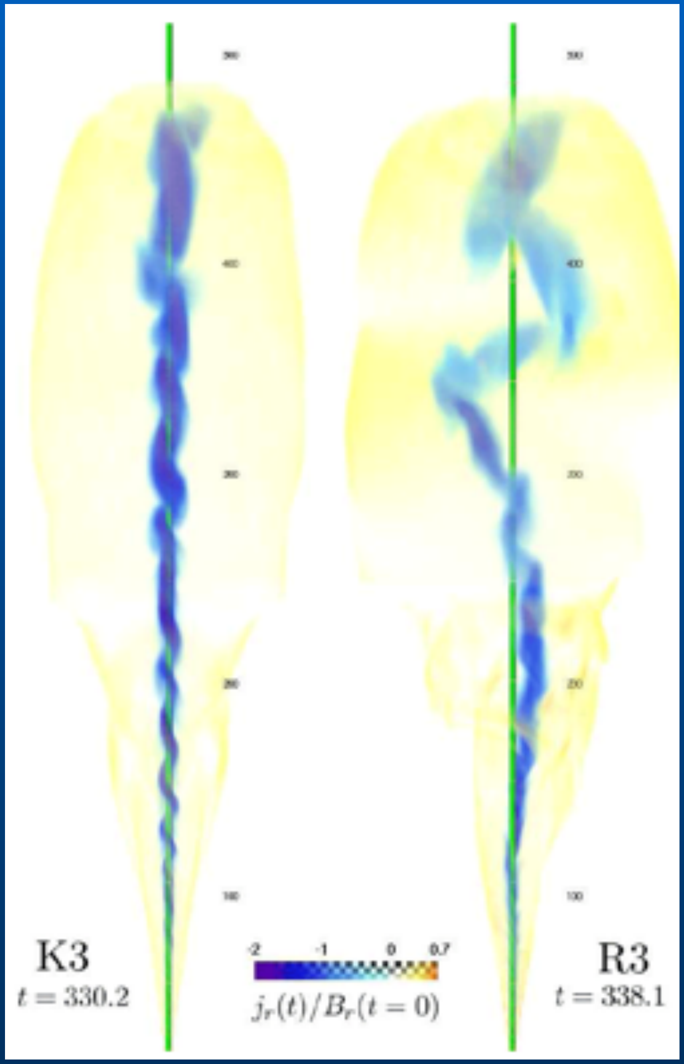
K3
$t = 330.2$
-2 -1 0 0.7
$j_r(t)/B_r(t=0)$
R3
$t = 338.1$

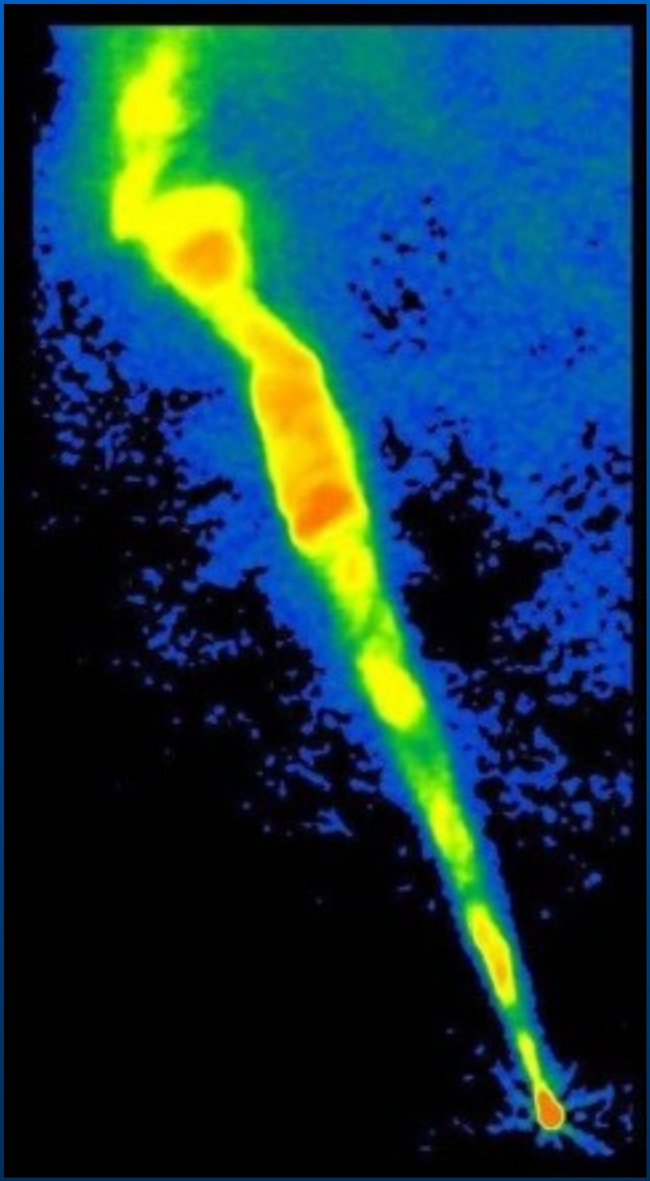

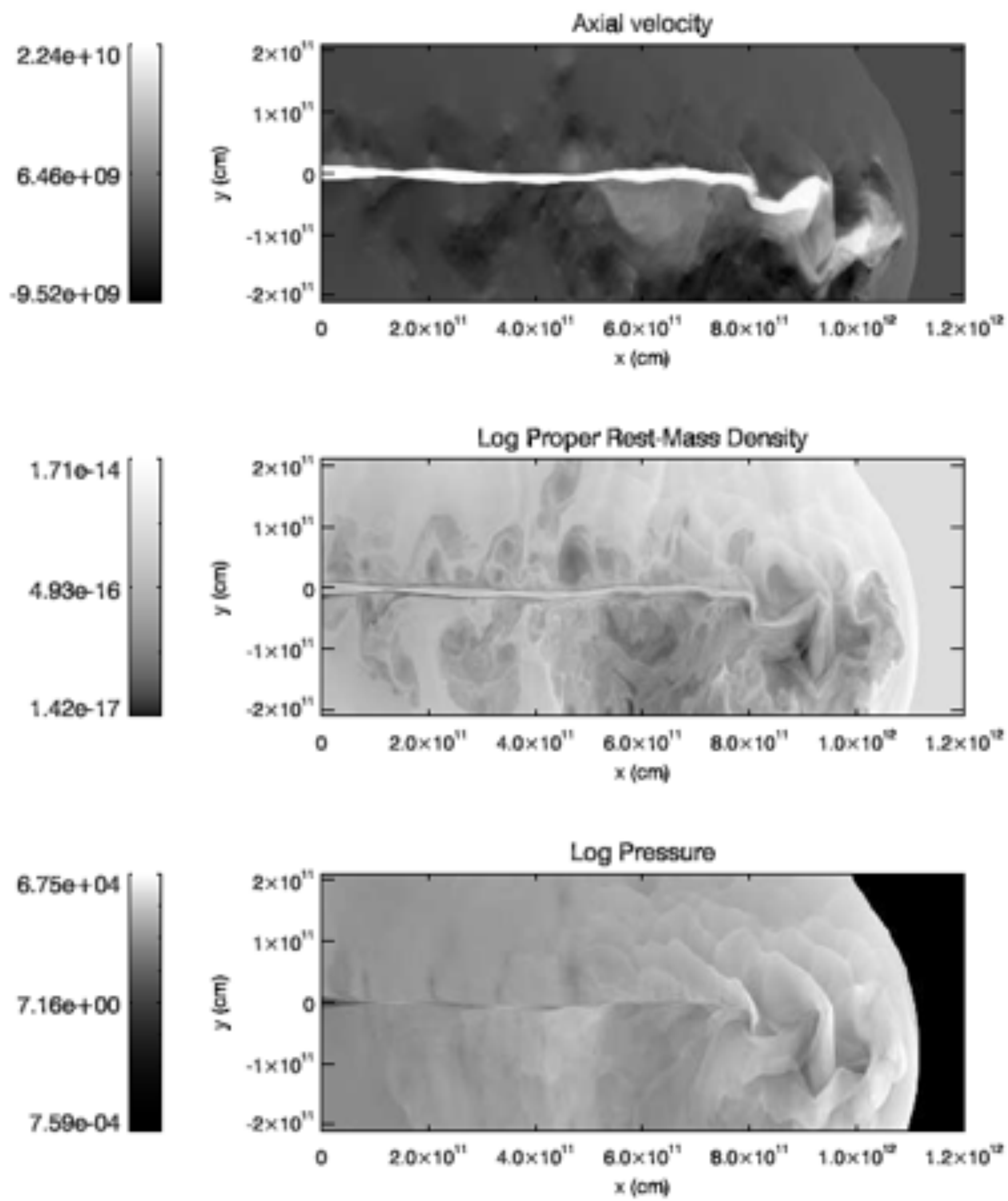
Axial velocity
2.24e+10
6.46e+09
-9.52e+09
y (cm)
x (cm)
Log Proper Rest-Mass Density
1.71e-14
4.93e-16
1.42e-17
Log Pressure
6.75e+04
7.16e+00
7.59e-04

Jet-cloud interaction

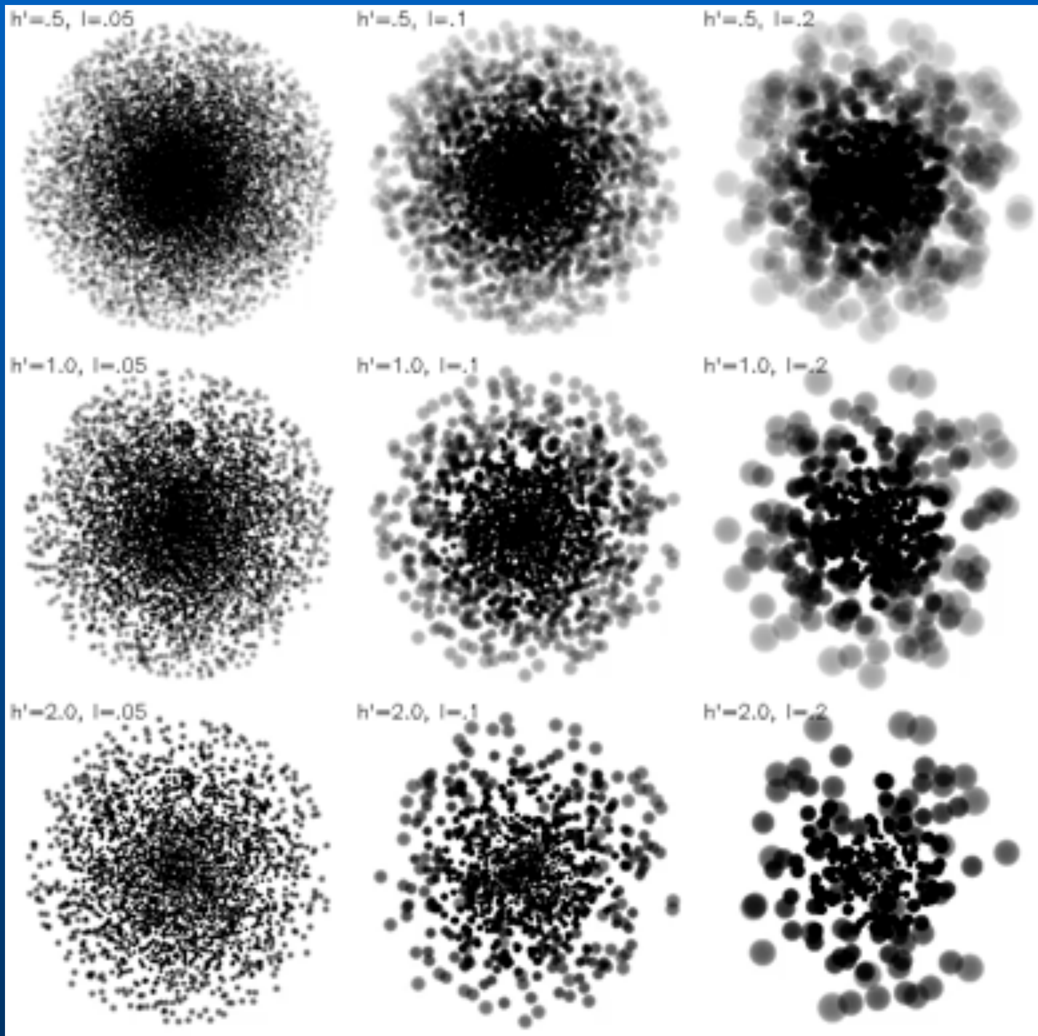

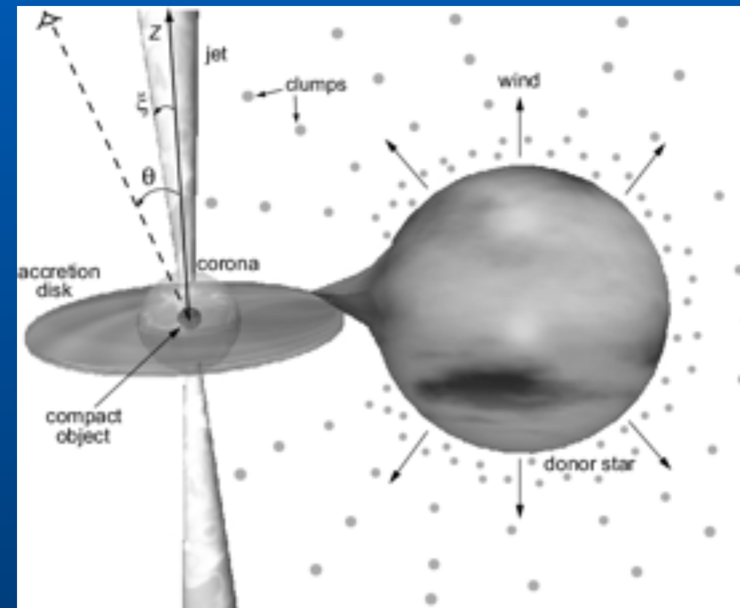

Jet-cloud interaction

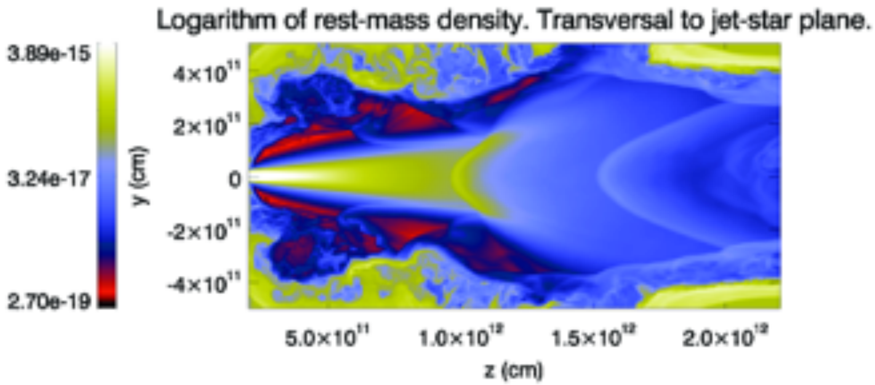

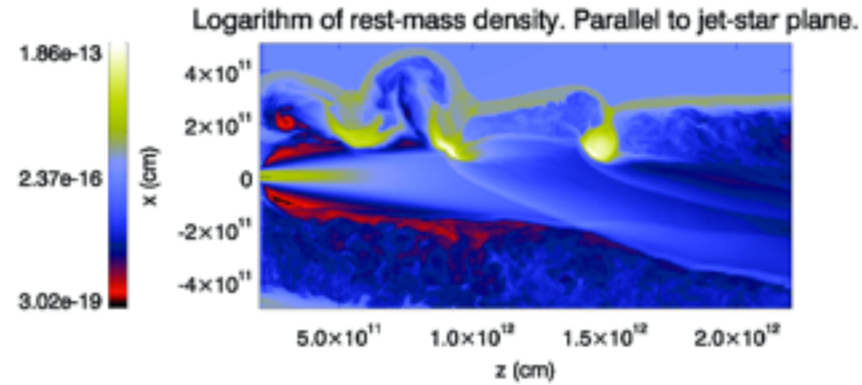

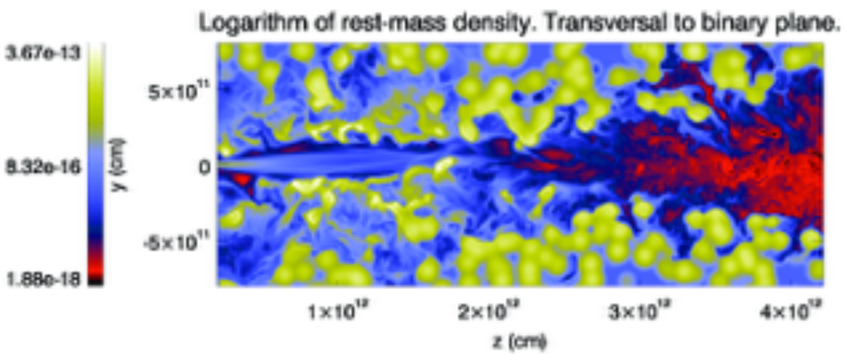

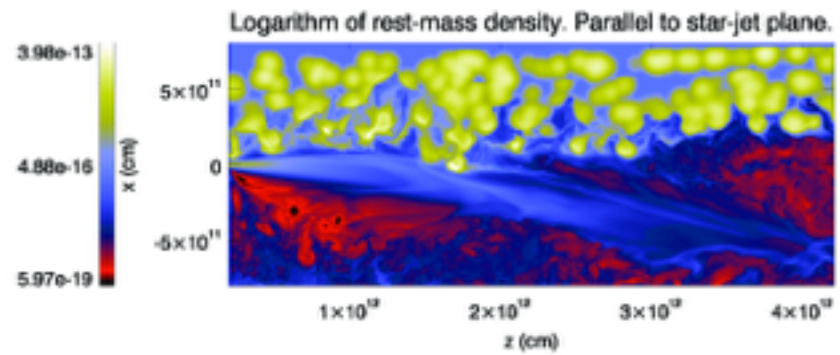

Jet-cloud interaction

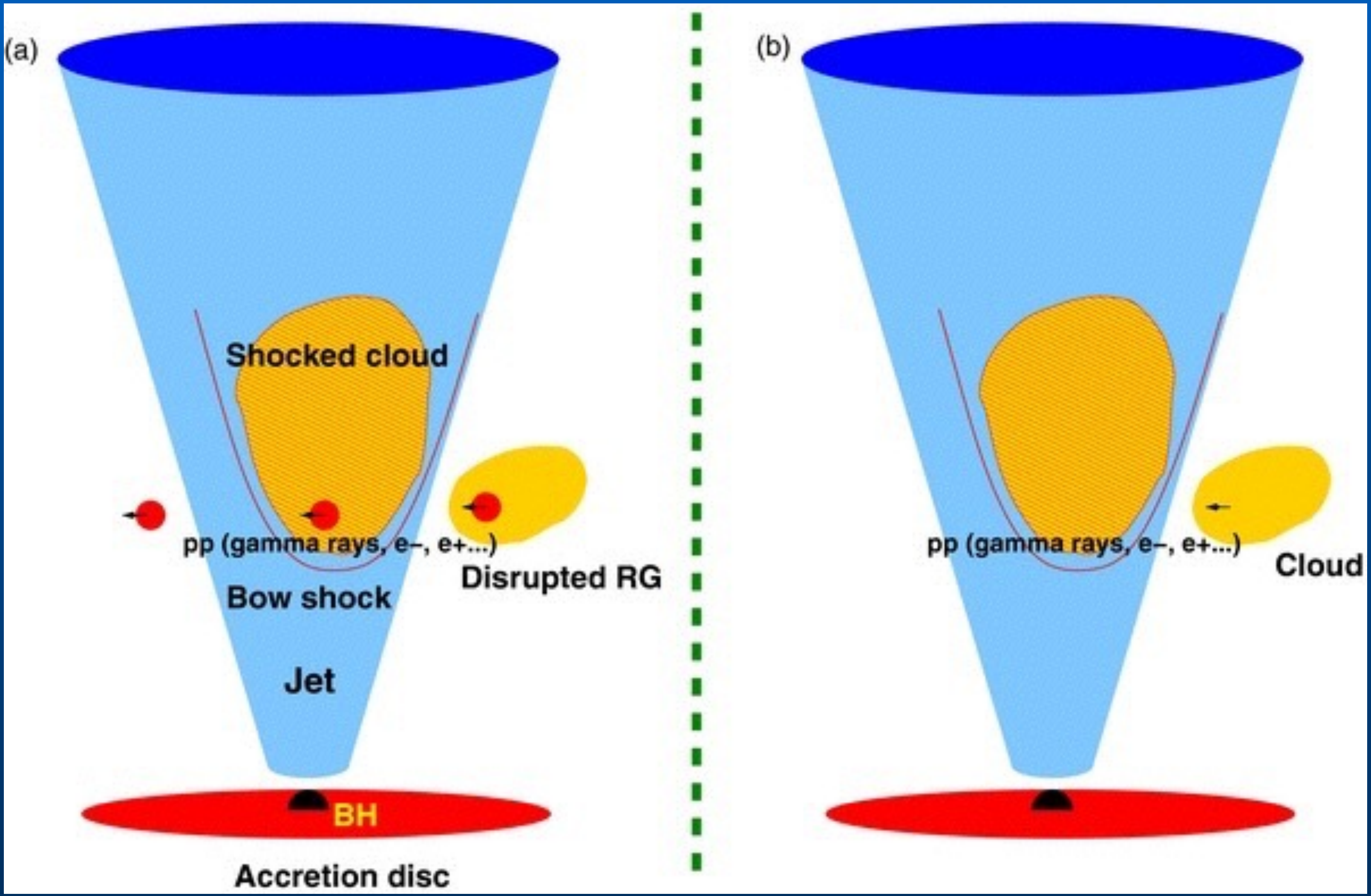

Jet-star interaction

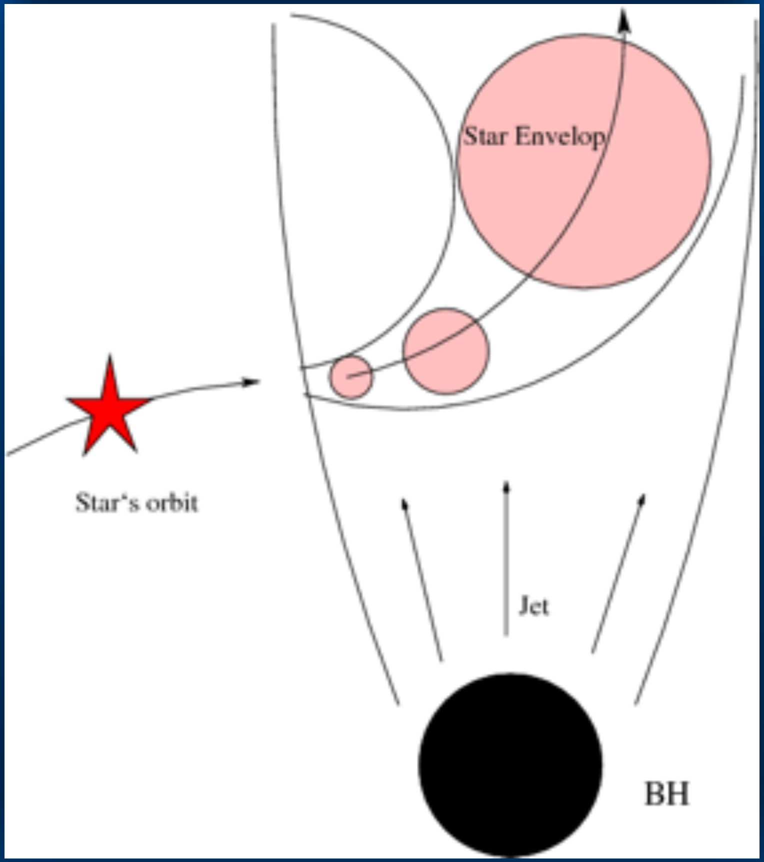

Jet-star interaction

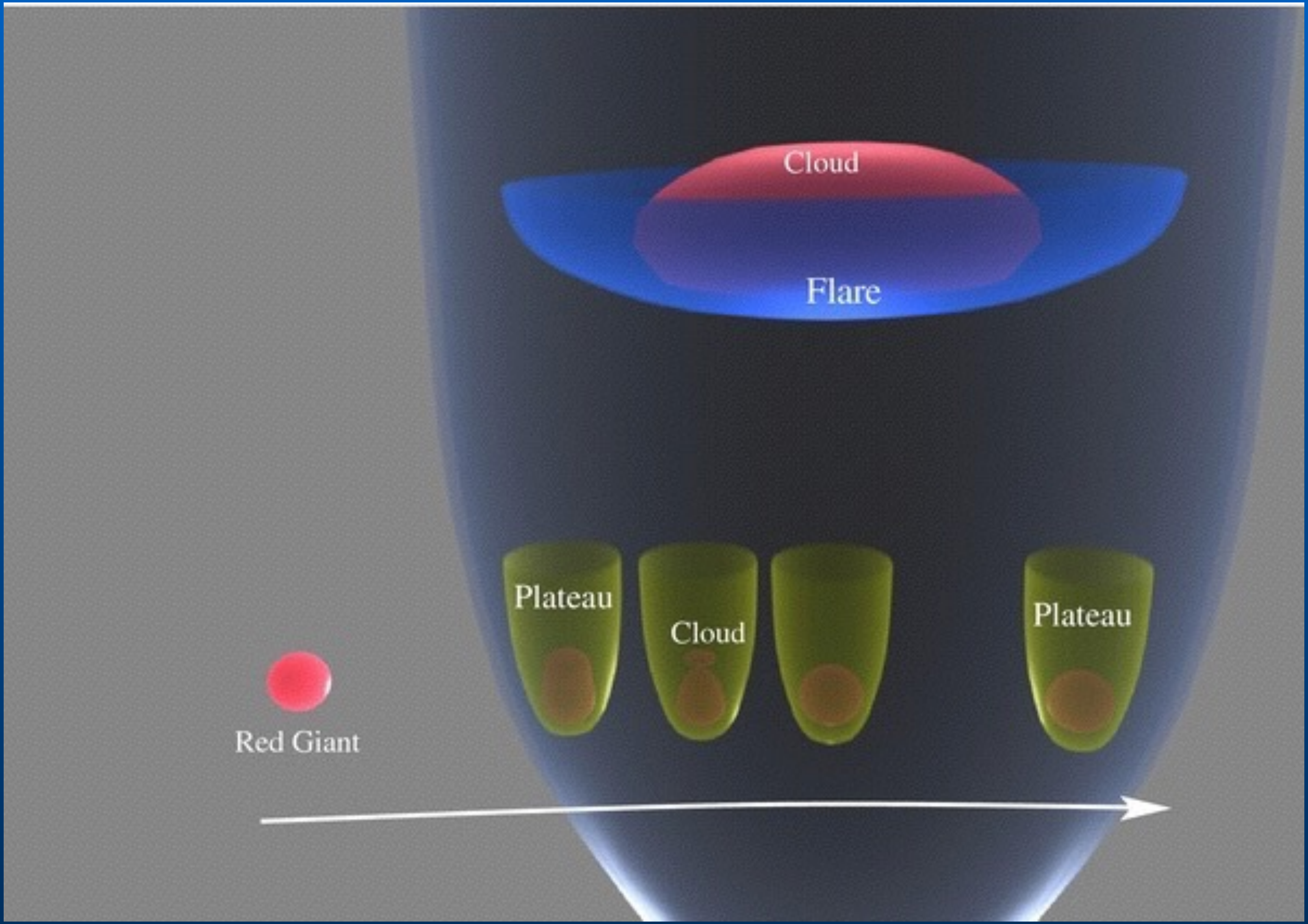

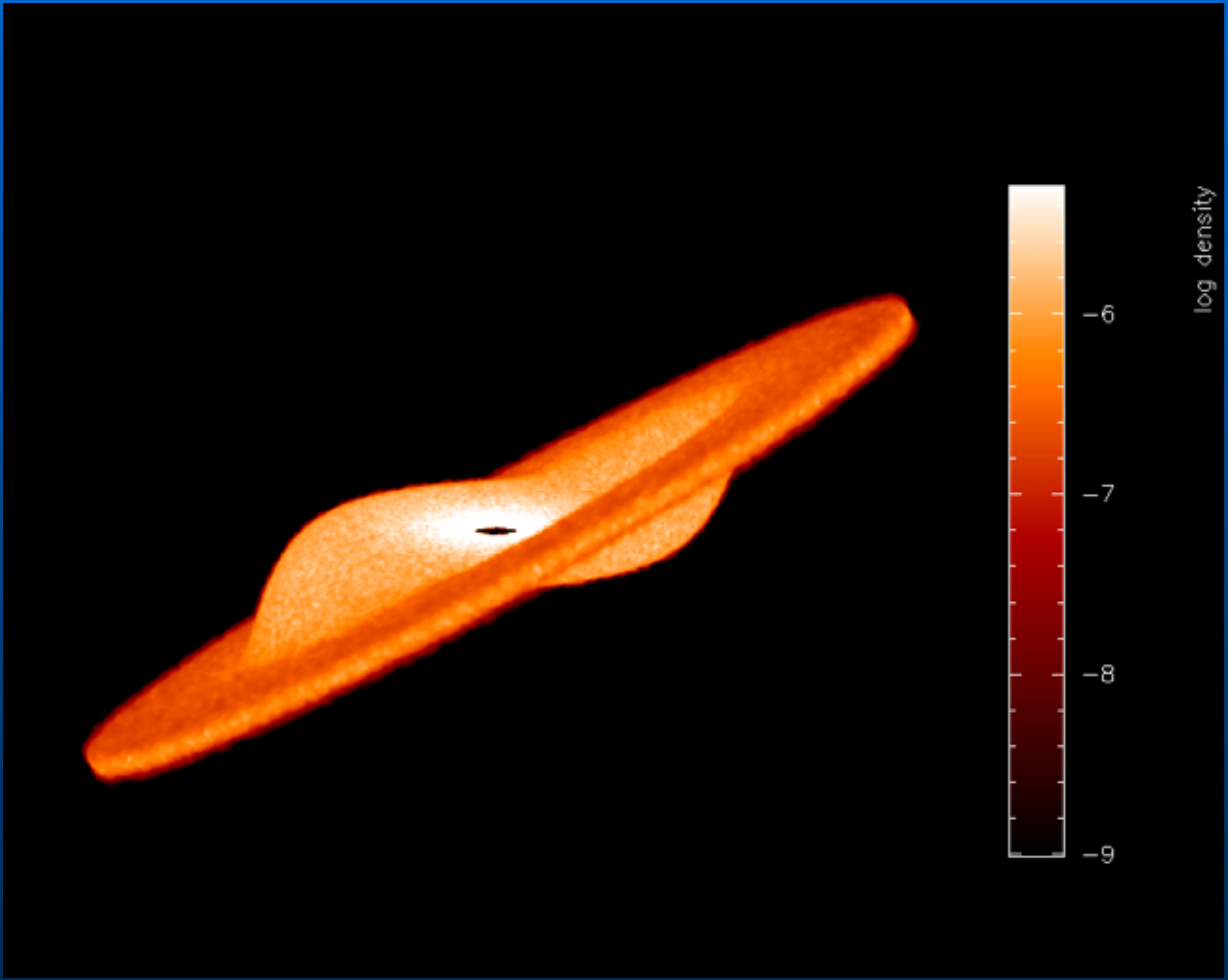

log density
−6
−7
−8
−9

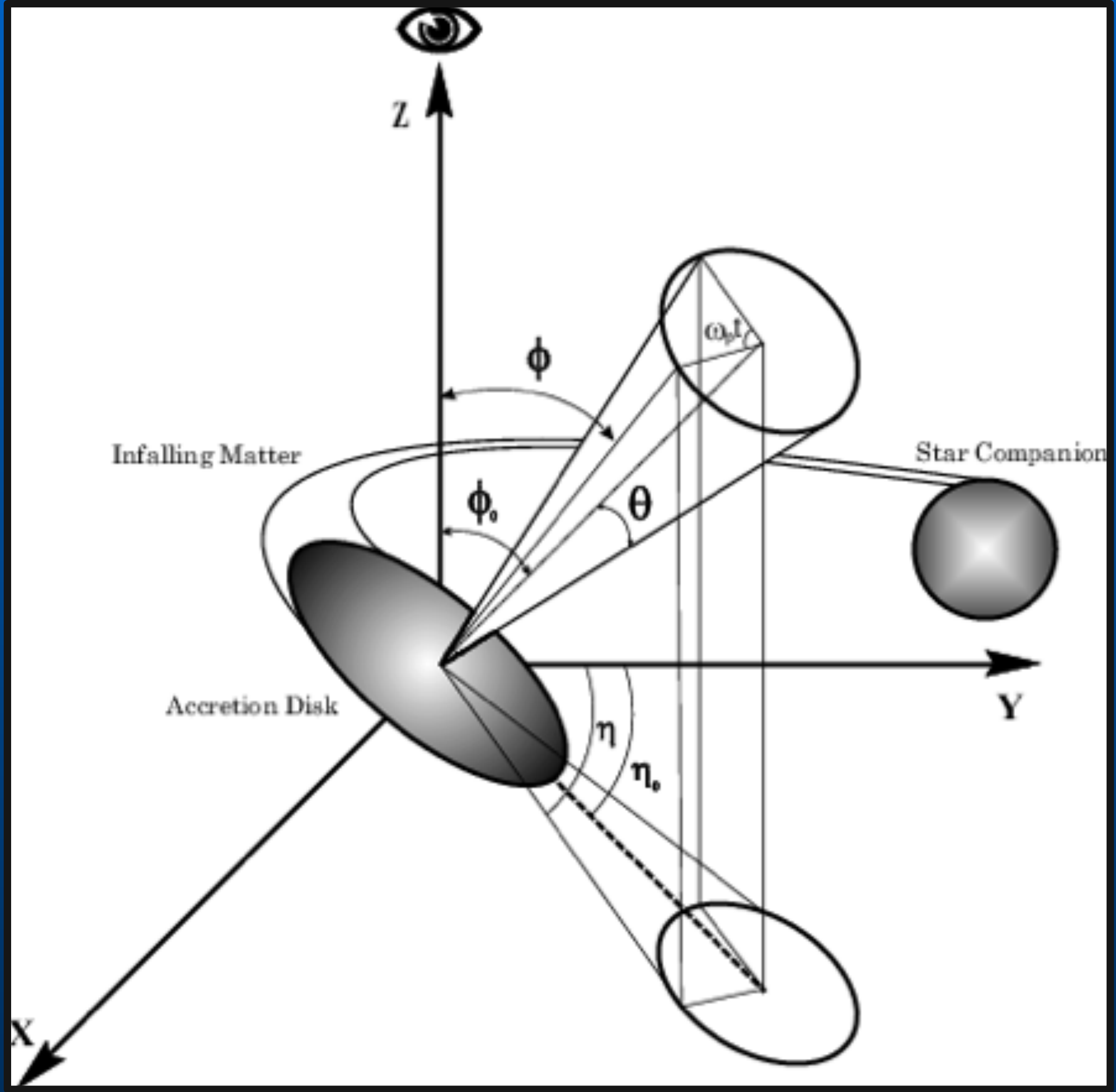
Z
ϕ
Infalling Matter
$\omega_p t$
Star Companion
ϕ_o
θ
Accretion Disk
Y
η
η_o
X

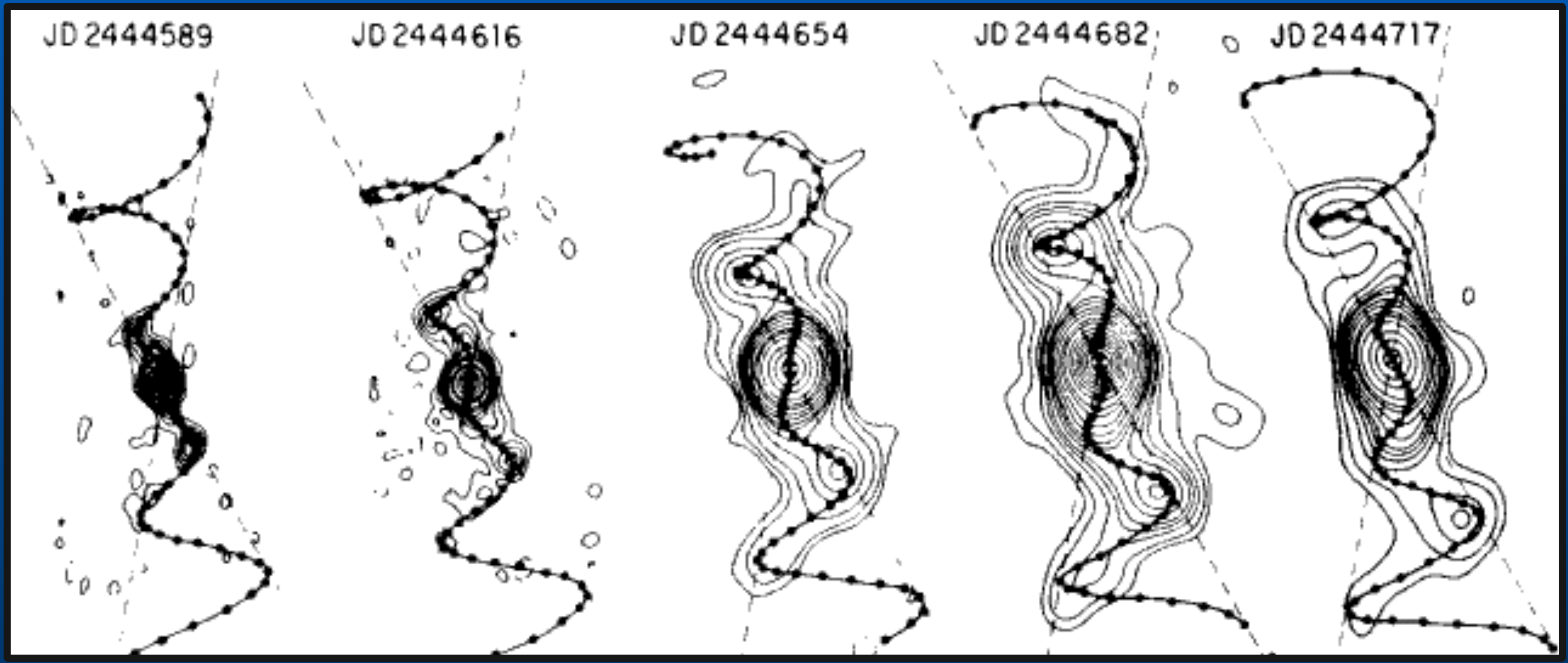
JD 2444589
JD 2444616
JD 2444654
JD 2444682
JD 2444717

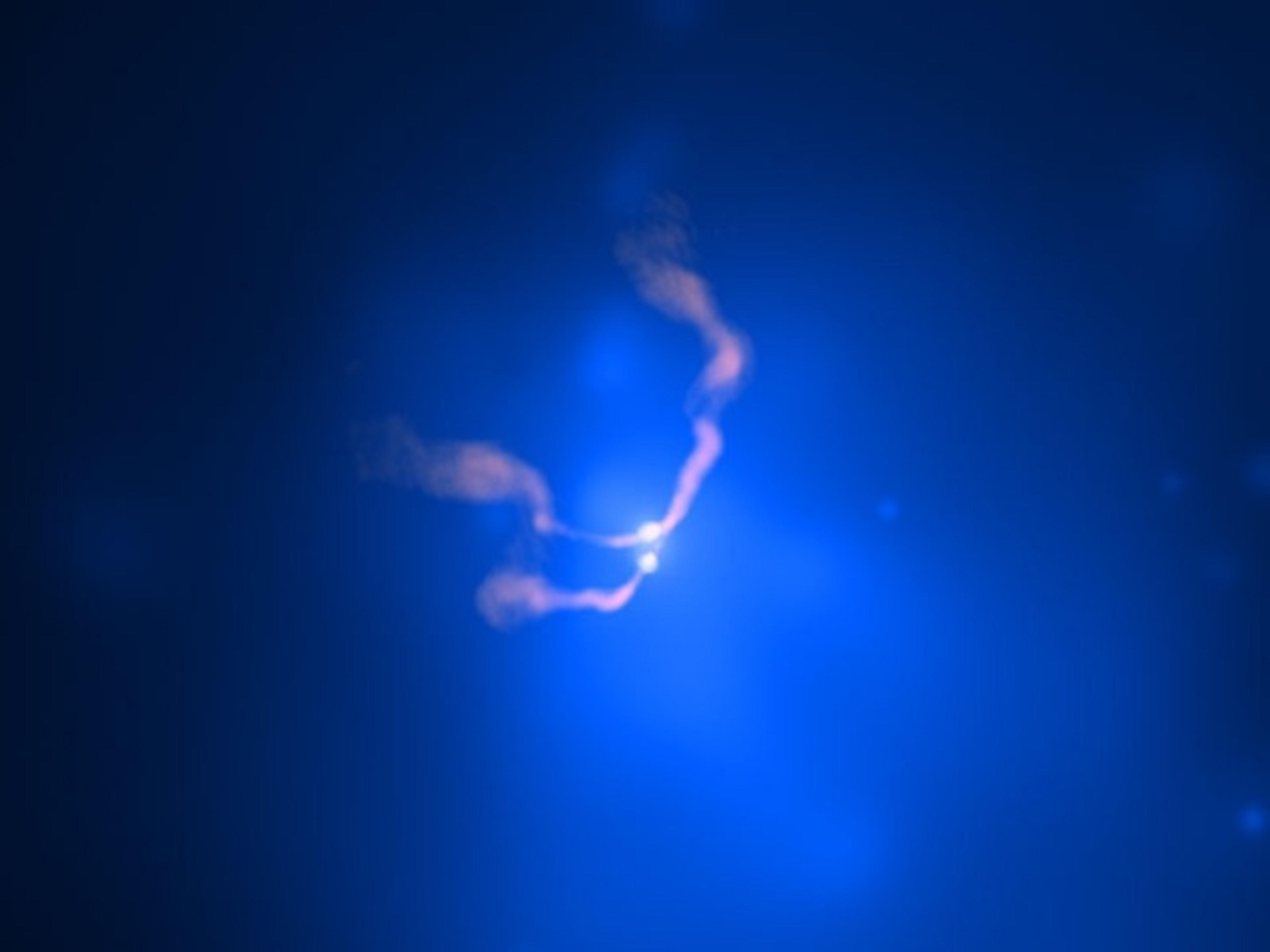

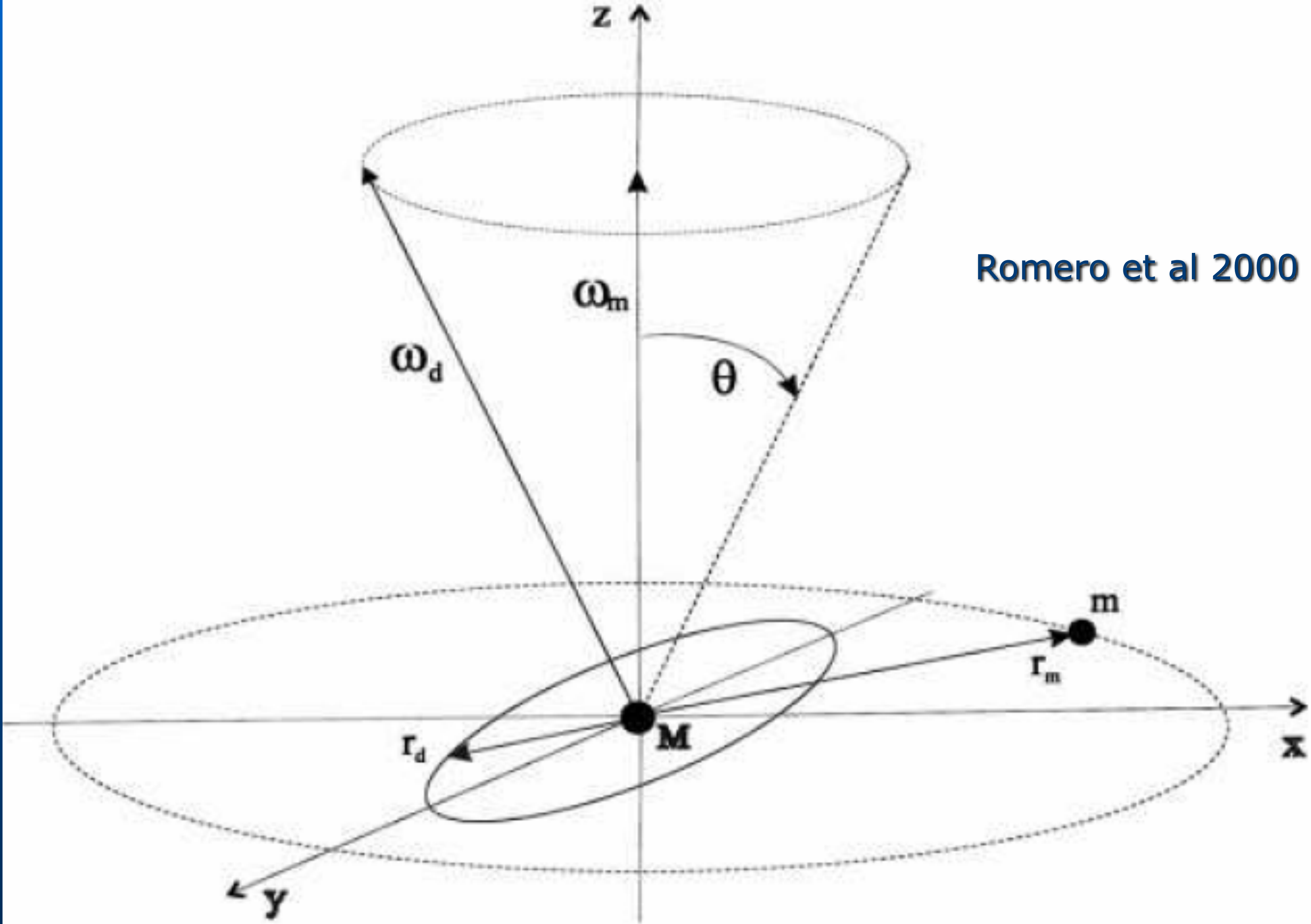

Romero et al 2000

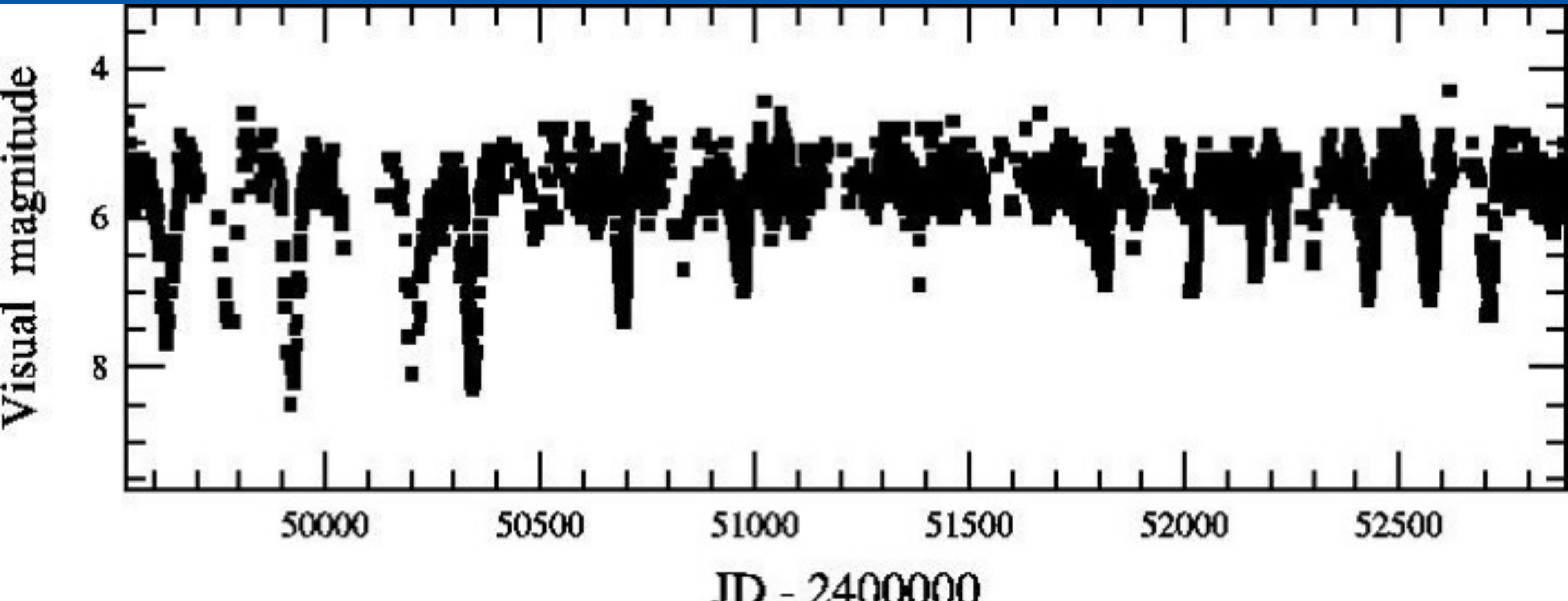
Visual magnitude
4
6
8
50000
50500
51000
51500
52000
52500
JD - 2400000